HHS Public Access

Author manuscript

Adv Drug Deliv Rev. Author manuscript; available in PMC 2017 February 01.

Published in final edited form as:

Adv Drug Deliv Rev. 2016 February 1; 97: 280–301. doi:10.1016/j.addr.2015.12.002.

Delivery of cancer therapeutics to extracellular and intracellular targets: Determinants, barriers, challenges and opportunities

Jessie L.-S. Au[a,b,c,d,*], **Bertrand Z. Yeung**[b], **Michael G. Wientjes**[a], **Ze Lu**[a], and **M. Guillaume Wientjes**[a]

[a]Optimum Therapeutics LLC, 1815 Aston Avenue, Carlsbad, CA 92008

[b]Department of Pharmaceutical Sciences, University of Oklahoma Health Sciences Center, Oklahoma City, OK 73014

[c]Medical University of South Carolina, Charleston, SC 29425

[d]Taipei Medical University, Taipei, Taiwan, ROC

Abstract

Advances in molecular medicine have led to identification of worthy cellular and molecular targets located in extracellular and intracellular compartments. Effectiveness of cancer therapeutics is limited in part by inadequate delivery and transport in tumor interstitium. Parts I and II of this report give an overview on the kinetic processes in delivering therapeutics to their intended targets, the transport barriers in tumor microenvironment and extracellular matrix (TME/ECM), and the experimental approaches to overcome such barriers. Part III discusses new concepts and findings concerning nanoparticle-biocorona complex, including the effects of TME/ECM. Part IV outlines the challenges in animal-to-human translation of cancer nanotherapeutics. Part V provides an overview of the background, current status, and the roles of TME/ECM in immune checkpoint inhibition therapy, the newest cancer treatment modality. Part VI outlines the development and use of multiscale computational modeling to capture the unavoidable tumor heterogeneities, the multiple nonlinear kinetic processes including interstitial and transvascular transport and interactions between cancer therapeutics and TME/ECM, in order to predict the *in vivo* tumor spatiokinetics of a therapeutic based on experimental *in vitro* biointerfacial interaction data. Part VII provides perspectives on translational research using quantitative systems pharmacology approaches.

Graphical Abstract

[*]Corresponding author at: Optimum Therapeutics LLC, 1815 Aston Avenue, Carlsbad, CA 92008; Tel: (760)438-1155; Fax: (760)438-1156; jau@optimumtx.com.

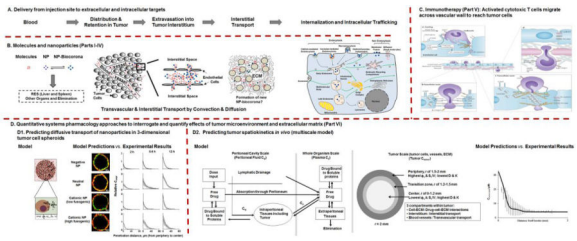

Keywords

Biointerfacial interactions; computational modeling; extracellular matrix; immune checkpoint therapy; interstitial and transvascular transport; intracellular trafficking; nanoparticles; RNAi; tumor microenvironment; tumor heterogeneities; spatiokinetics

1. Introduction

Advances in molecular genetics and medicine, nanotechnology and pharmaceutical sciences have broadened the scope of cancer therapeutic targets. In addition to tumor cells, components in the tumor microenvironment (TME) have emerged as clinically important targets. TME is a complex strcuture comprising cells, blood vessels, cytokines and extracellular matrix (ECM). The three major cell types in TME are fibroblasts, inflammatory/immune cells, and endothelial cells; these cells secrete or express cytokines and chemokines that interact with tumor cells [1]. ECM proteins, primarily collagen and fibronectin, are synthesized and deposited by fibroblasts, and represent a major fraction of larger tumors. Classes of cancer therapeutics include the traditional small molecules, macromolecules (e.g., proteins, antibodies), bioconjugates, viral vectors, and nanoparticle (NP) carriers (e.g., liposomes, micelles, and polymeric NP) [2]. These agents target tumor vasculature (e.g., anti-angiogenics), tumor interstitium (e.g., diagnostics or therapeutics targeting extracellular proteins), cell membrane (e.g., antibodies), and intracellular compartments such as the cytosol (e.g., RNAi, drugs targeting cytosolic proteins) [3–5] and nucleus (e.g., DNA gene vectors, DNA-active drugs) [6,7]. Their utility depends on their ability to reach their sites of action [8], which in turn is partly determined by TME and ECM. The goals of this report are to outline the processes and determinants of the delivery, transport and residence of cancer therapeutics and their NP carriers in solid tumors. The unique challenges and opportunities for nanomedicines, RNAi gene therapeutics and immune checkpoint therapy are also discussed.

As most cancer therapeutics are administered by intravenous injections, this review will focus on the transfer from blood to target sites. For the orally active agents such as tyrosine kinase inhibitors, additional processes governing the transport into the systemic blood, including absorption from the gastrointestinal tract and hepatic first pass elimination, are additional considerations.

This review comprises seven parts. Part I outlines the transfer processes of cancer therapeutics from the injection site to tumor interstitium, and Part II the processes from interstitium to cellular and intracellular targets; the barriers for delivery and the approaches

to overcome these barriers are summarized. Part III discusses the interactions of therapeutics with components of TME and ECM, e.g., formation of NP biocorona. Part IV outlines the challenges in animal-to-human translation of cancer nanotherapeutics. Part V is a review of immune checkpoint inhibitors, the newest therapeutic group with demonstrated clinical benefits in cancer patients, and a discussion of the potential roles of TME/ECM in determining their treatment efficacy. Part VI introduces the concept of using computational modeling tools to account for the dynamic changes in the properties of the therapeutics (e.g., protein binding, binding to targeted ligands) and for the spatial- and time-dependent changes in the tumor properties (e.g., intratumoral heterogeneities in vessel density and tumor cell density, growth- and treatment-induced changes). Examples of successful use of multiscale modeling to quantify the effects of the properties of therapeutics and tumors on the delivery and spatiokinetics of cancer therapeutics in tumors are discussed. Part VII provides perspectives on translational research using quantitative systems pharmacology approaches.

Most of the subject matters covered in Parts I and II have been well researched and multiple reviews, including several from our group, are available. Please see our earlier reviews [5,9–14] for more details and additional relevant references.

2. Part I. Delivery of cancer therapeutics from injection site to tumor interstitium

2.1. Processes

Figure 1 outlines the processes for the transfer of cancer therapeutics from injection site to tumor interstitium [5,9–14]. After a systemic administration (e.g., intravenous injection), a therapeutic undergoes elimination, e.g., *via* hepatic metabolism, renal excretion and degradation by enzymes in blood. Drug carriers such as lipid or polymeric NP are also subjected to surface opsonization and subsequent entrapment by the phagocytic system and cells in the reticuloendothelial system (RES, e.g., macrophages, Kupffer cells). Second, the delivery, transport and residence of the therapeutic to and at the target site involves multiple kinetic processes that in turn are determined by the properties of the therapeutic (e.g., size, surface charge, protein binding) and the tumor (e.g., blood flow, lymphatic drainage, tumor cell density, intratumoral pressure gradient, ECM).

2.1.1. Tumor blood flow—The following summarizes the transport of a therapeutic from the injection site to tumors *via* systemic blood circulation [5,9–14]. There are substantial differences in blood perfusion between tumors and normal tissues. In general, tumors show greater blood viscosity due to the presence of tumor cells and large molecules (e.g., proteins and collagen), and have more tortuous and less well organized blood vessels, producing the net result of a greater flow resistance and lower average blood flow. On the other hand, tumor vessels are more leaky due to the discontinuous endothelium and greater vascular permeability secondary to the elevated levels of vasoactive and growth factors. The distribution of blood vessels in a tumor is affected by the tumor size and is spatial-dependent. Small tumors (<2 mm) receive their blood supply from surrounding host tissues, whereas larger tumors are supported by newly formed microvessels. There is substantial intratumoral heterogeneity with respect to blood perfusion in solid tumors. A solid tumor

typically comprises three major regions: (a) avascular necrotic region with no vasculature, (b) semi-necrotic region containing capillaries, pre-and post-capillaries, and (c) stably perfused region containing many venous vessels and few arteriolar vessels. Larger tumors usually show lower density of blood vessels and cells in the center compared to the periphery and higher avascular-to-well-perfused area ratio and greater distance between capillaries. These heterogeneities contribute to uneven drug distribution within solid tumors and the lower weight-adjusted drug concentration in larger tumors. Because blood vessels are mainly veins/venules in the tumor interior and arteries/arterioles in the periphery, the blood flow, which is determined by the arteriole-venule pressure difference, is negligible in the interior and is greater in the periphery.

2.1.2. Extravasation—After entering a tumor, the therapeutic leaves the intravascular space to enter the interstitium (i.e., extravasation) [5,9–17]. This process is summarized below. The major pathway of transport across tumor microvascular wall is by extravasation *via* diffusion and/or convection through the discontinuous endothelial junctions, whereas transcytosis plays a relatively minor role. Transport of small molecules is mainly by diffusion, whereas transport of large molecules or particulates is mainly by convection. Diffusion depends on diffusivity and concentration gradients of the therapeutic, whereas convection depends on the fluid flow driven by hydraulic conductivity and pressure difference within the tumor. For example, transvascular fluid transport is driven by the hydrostatic pressure and by the osmotic pressure due to differences in the protein levels between intravascular and interstitial space. Leakiness in tumor vessels enhances diffusivity and hydraulic conductivity and thereby promotes extravasation. But this, together with interstitial fibrosis and interstitial space contraction caused by stromal fibroblasts in solid tumors, also elevates the interstitial fluid pressure (IFP) and reduces transvascular fluid transport and extravasation. After extravasation, drugs or particulates move through interstitial space to reach tumor cells located distal to blood vessels.

2.1.3. Interstitial transport—Two major components of a solid tumor are tumor cells and ECM. Both constitute significant barriers to interstitial transport [5,9–14].

ECM comprises fibrous proteins (e.g., collagen, elastin) and polysaccharides (e.g., hyaluronan, glycosaminoglycan) [18]. These proteins are a source of physical resistance to diffusional transport and are associated with lower hydraulic conductivity and lower convective flow in interstitium. Collagen appears to contribute more to transport resistance compared to glycosaminoglycan or hyaluronan, e.g., diffusion coefficient of IgG is inversely related to the collagen content in a tumor. Enzymes that degrade tumor ECM materials, such as collagenase and hyaluronidase, promote intratumoral dispersion of small molecules, macromolecules (e.g., monoclonal antibodies) and NP (e.g., liposomes); collagenase is more effective for larger molecules and NP whereas hyaluronidase is more effective for smaller molecules such as doxorubicin [5,19–22]. Of note is that collagenase also promotes T cells penetration in tumors, which may have relevance in immunotherapy (see Part V).

Binding of drugs or their NP carriers to ECM and cell membrane (e.g., receptors) reduces the unbound drug/NP concentration available for interstitial transport. The binding barrier is more significant for active targeting NP due to the high specificity and affinity between the

targeting ligand and receptors [5,23]. This property is likely to affect the formation of biocorona on NP and consequently the transport and residence of NP in tumors (see Part III).

2.1.4. Tumor lymphatic drainage—The lymphatic system, which is responsible for clearing macromolecules and large particles and returns the interstitial fluid into the blood circulation, is impaired in solid tumors. This poses two opposing effects on therapeutic delivery and transport: reduces clearance from tumor interstitium but also limits the fluid flow and thereby retards convection-mediated extravasation and interstitial transport (see Extravasation) [5,9–14].

2.2. Approaches to improve delivery, interstitial transport and retention of therapeutics in solid tumors

Various approaches have been evaluated [5,9–14].

2.2.1. Enhance blood-to-tumor transport and extravasation—Approaches to improve drug delivery to tumors include the following. (a) Modulation of intratumoral pressure gradients to promote extravasation. This is accomplished by elevating the microvascular pressure using angiotensin II, or decreasing IFP using physical methods (e.g., hyperthermia) and chemical methods (osmotic agent mannitol) [24–28]. (b) Targeting tumor vasculature by using cationic NP. The cationic NP, through electrostatic interactions, localize on the luminal endothelial membrane of blood vessels [29–31] and are preferentially (15–30 times higher) taken up by angiogenic tumor endothelium relative to normal tissues [32]. This approach provides greater tumor delivery relative to the passive EPR targeting [33]. Selective targeting of tumor vasculature is further achieved by conjugating NP with tumor endothelium specific ligand, e.g., integrin $\alpha_v\beta_3$ [34,35]. (c) Normalization of tumor vasculature using pharmacological approaches (topoisomerase II inhibitor, anti-angiogenic agents). The normalized vasculature is less permeable, less dilated, less tortuous, and shows more normal basement membrane and greater pericyte coverage. However, these changes are associated with decreased IFP and increased tumor oxygenation, produce unpredictable outcome, reduce the capillary pore size to limit the extravasation of small NP (<20 nm), and do not improve the delivery of liposomal doxorubicin (85 nm). In addition, benefits from normalization are transient due to vascular cell apoptosis and the resulting reduced vessel density [12,36–39]. (d) Enhance extravasation using vasodilators such as nitric oxide-release agents, nitroglycerin, angiotensin converting enzyme inhibitors, or prostaglandin E1 agonist [40–47]. (e) Enzymatic degradation of ECM (e.g., collagenase, hyaluronidase). (f) Tumor-priming using cytotoxics to transiently increase interstitial space (e.g., tumor necrosis factor-α, paclitaxel, radiation) (see also 2.3.3).

2.2.2. Passive targeting *via* enhanced permeability and retention—Solid tumors have two properties that favor drug/particulate accumulation and retention in tumors, i.e., leaky tumor blood vessels allow large molecules to extravasate whereas defective lymphatic drainage decreases the clearance of compounds from tumor interstitium, referred to as the enhanced permeability and retention (EPR) effect [47,48]. For EPR, retention plays a larger role relative to extravasation. EPR is predominant for compounds with molecular weights larger than 40 KD but negligible for smaller molecules that readily redistribute to blood

circulation *via* diffusion and/or convection. EPR is affected by the tumor size with a greater EPR in smaller tumors [47]. This is likely because of the greater vessel density allowing for more extravasation in smaller tumors compared to larger tumors with greater fractions of avascular regions [5,9–14].

2.3. Unique issues for nanomedicines

Nanotechnology has emerged as an important tool in cancer translational research. NP pose several advantages: (a) improve the solubility of hydrophobic compounds, (b) protect a molecule from undesirable interactions with biological milieu components (e.g., reduce its metabolism or degradation), and (c) favorably alter the distribution and provide passive targeting of solid tumors due to the EPR effect [5,47,48]. NP can be used to deliver diagnostics and therapeutics, including small and large molecules, gene vectors, and biosensors, to tumor interstitium, cell membrane, or intracellular compartments [5]. As NP are versatile and can be made of different types of materials, and can have different sizes, surface charges, and surface modifications, there is the potential to tailor the design of NP for their intended functions [5]. On the other hand, the properties of NP affect its delivery to tumors, as follows.

2.3.1. Effects of nanoparticle properties on blood-to-tumor transfer—The NP size determines its extravasation from blood vessels, with the capillary pore size posing as the upper size limit [5,10,12,14]. After extravasation, the smaller NP are widely dispersed and show deeper penetration in the interstitium relative to larger NP that are localized in peri-vascular space [49]. Generally, a size of less than 200 nm is favorable for extravasation as well as interstitial transport. Surface charge of NP is another important determinant. The general view is that surface charge affects the NP clearance from systemic circulation, in part due to interactions with blood components (e.g., immunoglobulins); resulting in surface opsonization and subsequent entrapment in the RES system that resides predominantly in liver and spleen [50,51]. For example, cationic liposomes are rapidly eliminated by the RES system, a property that limits their efficacy and utility as a delivery vehicle [52]. In vitro studies show that negatively charged NP are removed by macrophages [53], suggesting their susceptibility to RES clearance. The types, quantities and conformations of the opsonins are determined by NP chemistry. Similarly, interactions of positively- or negatively-charged NP with ECM components may hinder their penetration and dispersion in tumor [54].

Surface modifications using hydrophilic and flexible polyethylene glycol (PEG) and other surfactant copolymers (e.g., poloxamers, polyethylene oxide) limit the protein absorption on the particle surface and thereby provide stealthness and protect NP against RES entrapment and prolong the NP circulation time [5,11,55–57]. On the other hand, pegylation may neutralize the positive surface charge that facilitates endocytosis, and high affinity binding to cell surface receptors may limit the interstitial transport [5,11,58].

2.3.2. Approaches to enhance nanoparticle delivery to tumors—Approaches aiming at improving the delivery of NP therapeutics to their intended targets include some of the approaches listed in the above sections, and some approaches that derive from the known

effects of selected NP properties. An example of the latter is the use of the RES entrapment feature to target siRNA delivery to the liver [59,60].

2.3.3. Tumor priming to promote extravsation and interstitial transport—Tumor priming refers to using apoptosis-inducing agents to promote tumor transport and is based on the following observations. Our group made the observation in a 3-dimensional *in vitro* model (i.e., animal tumor fragments) that paclitaxel, by inducing apoptosis, reduces tumor cell density and increase the fraction of interstitial space, and thereby promotes its own interstitial transport; the same was observed for doxorubicin [9,61]. This tumor fragment model is devoid of blood or fluid flow and therefore does not involve convective transport. Hence, our finding indicates tumor priming significantly enhances the drug diffusivity. A separate study by another group using an *in vivo* model found that paclitaxel apoptosis leads to vessel decompression [62]. We next used a combination of *in vitro* and *in vivo* models to demonstrate that a minimum level of about 10% drug-induced apoptosis is required for tumor priming to be effective [10,63]. Under *in vivo* conditions, apoptosis-inducing paclitaxel treatments produced a transient increase (from 24 to 96 h) in interstitial space or porosity that led to (a) expansion of patent vessels and blood-perfused area (without affecting the vessel length or density), resulting in greater extravasation of NP, and (b) higher diffusivity and hydraulic conductivity, resulting in greater interstitial transport; these tumor structural changes collectively promoted the delivery and intratumoral dispersion and the efficacy of pegylated liposomal doxorubicin (85 nm diameter) [63,64]. The tumor-priming effects, due to the higher susceptibility of tumor cells to apoptosis, are tumor-specific and not observed in normal tissues [5,64]. In a more recent study, paclitaxel tumor priming was found effective in promoting the delivery and transfection efficiency of siRNA therapeutics injected intraperitoneally or intravenously [65,66]. The effectiveness of tumor priming using paclitaxel or other apoptosis-inducing agents has since been verified by several other laboratories [67–70].

3. Part II. Delivery of cancer therapeutics to cellular and intracellular targets

Please see our earlier reviews for additional details and references [5,9–14]. Figure 2 shows the steps in the transport of a therapeutic from extracellular space to intracellular targets: (a) attachment to cell membrane through non-specific or specific binding, which in general facilitates the subsequent internalization, (b) internalization by endocytosis (followed by release from endosomes), membrane fusion, or diffusion, (c) transport in cytoplasm to intracellular cytoplasmic organelles or nucleus. A fraction may be released back to the extracellular space *via* exocytosis. Each of these processes are controlled by multiple factors, with additional and different determinants for NP, as follows [5,12,58].

3.1. Cell surface binding

Non-specific binding of a therapeutic to cell surface occurs due to electrostatic interactions, e.g., long-range van der Waals forces, short-range Born repulsive forces resulting from overlapping electron clouds, steric repulsive forces induced by the cell membrane surface glycocalyx, electrostatic double layer forces resulting from counterions attracted by the cell membrane surface potential, entropic protrusion and undulation forces arising from

molecular fluctuations of hydrocarbon chains, and hydrophobic forces due to loss of hydrogen bonding [5,71–73]. Positively charged molecules/NP show higher cell binding and internalization compared to neutral or negative entities. Surface modifications of NP such as pegylation and formation of biocoronae (due to interactions with proteins in biological milieu, see Part III) reduces the positive surface charge and alters cell binding [74].

Surface-modifications with targeting ligands enhance NP attachment on tumor cells. Specific binding to receptors or antigens on cell membrane surface is achieved by using targeting ligands, including antibodies, peptides, proteins, small molecule receptor ligands and carbohydrates [5,9–14,75]. The most popular ligands are monoclonal antibodies or Fab fragments specific to tumor cell antigens [76–78], peptide [79], folate [80], and transferrin [81,82].

3.2. Internalization

Internalization of therapeutics depends on multiple factors. Please see our earlier reviews for additional references [5,9–14]. Cell membranes are semi-permeable to small, hydrophobic or unionized molecules, which enter cells by passive diffusion. Larger, polar or charged molecules may enter cells by facilitated diffusion with the help of channel proteins in the membrane. Some molecules use ATP-dependent active transport to enter cells against the concentration. For larger molecules or NP carriers that cannot directly cross the plasma membrane, their uptake into cells is mediated by endocytosis, which involves a complex coordination of events leading to different intracellular transport pathways and the deposition of molecules/NP in different subcellular organelles [83–85]. The major mechanism of molecule/NP internalization is clathrin-mediated endocytosis, which recruits the molecule/NP-binding cell surface receptors and involves the formation of coated membrane invaginations on plasma membrane (about 2% of total area) [5,86,87]. Other less prominent endocytosis mechanisms include (a) caveolae-mediated endocytosis that involves caveolin-1-expressing structures (which include 500–100 nm flask-shape invaginations on membrane, large neutral pH intracellular structures, small vesicles and tubules); the endocytosed molecule/NP are located, after leaving cell membrane, in caveolar vesicles that later fuse with either caveosomes in the cytosol or early endosomes [5,88], (b) clathrin- and caveolae-independent endocytosis that is dependent on cholesterol [89], (c) a second cholesterol-dependent pathway, macropinocytosis, which is involved in fluid-phase endocytosis and where the endocytosed molecule/NP are located in macropinosomes [90]. Fluid phase endocytosis is a low-efficiency and nonspecific process, is primarily driven by the extracellular concentration, and is less prominent compared to other absorptive and receptor-mediated endocytosis processes. Macropinocytosis occurs in cells with active membrane or cytoskeletal (e.g., actin) activity. Liposomal NP also use non-endocytic pathways such as membrane fusion, a process that depends on the cholesterol in the liposome and cell membrane, resulting in the release of the NP contents into the cytosol [5,91,92].

The various endocytosis pathways show different upper particle size limits, i.e., 200 and 500 nm for clathrin- and caveolae-mediated endocytosis and up to 5 μm for macropinocytosis.

3.3. Endocytic transport

The complex network and regulation of endosomal transport have been extensively studied; readers are directed to several excellent reviews on this subject matter [93–98].

3.3.1. Endosomes—The endocytosed cargo and membrane vesicles, after uncoating, fused with early endosomes [99]. Early endosomes is the sorting center where the internalized materials are sorted to different pathways that involve three types of endosomes, i.e., early, late and recycling endosomes, with distinct markers (Rab5, Rab7, and Rab11, respectively). These processes are as follows. (a) Early endosomes lose the proteins responsible for recycling and eventually become late endosomes. This process is associated with membrane proton pump V-ATPase activity that causes proton influx and a continuous pH drop from 6.2–6.3 in early endosomes to 5.0–5.5 in late endosomes. The late endosomes move to perinuclear area where they fuse with each other or with lysosomes that are even more acidic (pH 4.8–5.4) and contain various enzymes that degrade the cargo. (b) Some materials are sorted into intraluminal vesicles (ILV) formed by the budding of endosomal membrane into the endosomal lumen. The resulting multivesicular bodies (MVB) are formed during the maturation of early endosomes to late endosomes. ILV are subjected to two fates: ILV are released into the extracellular space as exosomes when MVB fuse with the cell membrane or are degraded when MVB fuse with lysosomes [100] (c) Transport in recycling endosomes back to the cell membrane. (d) Transport *via* the trans-Golgi network to either lysosomes or recycle back to the Golgi [101–103].

3.3.2. Endocytic recycling—The removal of membrane proteins and lipids from the cell surface by endocytosis is balanced by endocytic recycling that returns these materials to the cell surface.

The recycling process is complex, and involves GTPases (Rab proteins) and various signaling pathways that regulate the sorting of molecules/proteins and the trafficking of vesicles. The two types of recycling pathways are recycling of cargo internalized by clathrin-dependent endocytosis (CDE) or by clathrin-independent endocytosis (CIE). CIE typically refers to internalization of cargo *via* caveolar endocytosis. The recycling of classic CDE cargo proteins such as transferrin and low density lipoprotein appears to occur by default without needing specific cytoplasmic sequences for recognition and sorting, whereas the recycling of CIE cargo and signaling receptors involves a selection process [93,104]. Both pathways require Rab11 function, and cells deficient in Rab11 exhibit a 1.5-fold reduction in lipid NP uptake, presumably due to decreased recycling of regulators necessary for entry [105].

Recycling can occur quickly or slowly. For example, NP appear in recycling endosomes within 1 h after endocytosis [105]. The fast recycling route goes from early endosomes back to the plasma membrane. The slow recycling route involves the transport of cargo from early endosomes to endosome recycling compartment (ERC) and then from ERC to plasma membrane [104]; the transport to ERC requires proteins such as nexins responsible for sorting cargo to recycling endosomes, and the absence of these proteins triggers the degradation of CDE cargo such as transferrin by late endosomes or lysosomes.

The current prevailing model is that during endosomal maturation, parts of the early endosome form tubular structures that become ERC whereas the remaining main body becomes MVB. In most cells, ERC is localized near the microtubule organizing center and Golgi complex, and the ERC tubules involved in the CIE recycling align along the microtubules, facilitating the actin- and microtubule-dependent transport of recycled vesicles to the cell membrane.

3.3.3. Intracellular release—For drugs or drug-loaded NP that act on targets in the cytosol or the nucleus, their effectiveness depends on their release from endosomes. An example is the gelonin-based immunotoxins that, regardless of their targeting or trafficking properties (e.g., different antigens, different antigen densities, different binding affinity to tumor cells), were equally effective after normalizing to their release from endosomes; this finding indicates endosomal release instead of internalization, is the determinant of intracellular delivery [106]. Endocytic escape of NP is highly dependent on its physical characteristics (e.g., size, zeta potential) and its chemical composition (e.g., fusogenic lipids, antibody conjugation) (see section 3.6.2 for more discussion).

3.4. Cytosol-to-nucleus translocation

Drugs or NP transit from the cytosol to the nucleus *via* several mechanisms [5]. Smaller molecules (up to 9 nm, <50 kDa) can cross the nuclear envelope through the aqueous channel of the nuclear pore complexes *via* passive diffusion [107,108], whereas larger molecules, e.g., DNA, may enter the nucleus during mitosis when the nuclear membrane breaks down. Another mechanism is an active, energy-dependent nuclear transport that requires the presence of specific targeting sequences, e.g., nuclear localization signals, that mediates the interaction of molecule/NP therapeutics with transport proteins such as importins [5,109–112]. The third mechanism is the fusion of therapeutic-loaded endosomes with the nuclear membrane.

3.5. Unique issues for RNAi gene therapeutics

RNA interference (RNAi) by small interfering RNA (siRNA) or microRNA produces post-transcriptional gene silencing and represents a promising approach to correct faulty genes [11,113]. RNAi is mediated through the cytosolic RISC (RNA induced silencing complex). Briefly, the guide strand of the dsRNA is recognized and loaded onto RISC by the slicing protein Argonaute 2 (Ago2) while the passenger strand is cleaved and released, resulting in an activated form of RISC with a single strand RNA (guide siRNA) that directs the target mRNA recognition through complementary base pairing [114]. Ago2 then cleaves the target mRNA between bases 10 and 11 relative to the 5’ end of the siRNA antisense strand, and thereby causes mRNA degradation and gene silencing [11,115–120].

siRNA has unfavorable properties for the transport from injection sites to tumors, as naked siRNA are readily degraded by serum endonucleases and rapidly cleared by glomerular filtration, resulting in short plasma half-life of less than 10 min [121–124]. These problems are partially overcome by chemical modifications of the RNA backbone and use of NP carriers [11,60,121,125]. For entering cells, naked siRNA do not readily cross the cell membrane, again due to the high molecular weight, large size and negative charges of the

phosphate backbone. These concerns have led to the use of NP carriers; cationic pegylated liposomes are a popular choice [11].

The major mode of internalization of siRNA-NP is endocytosis. For example, the complex of siRNA and positively charged liposomes (lipoplex) interacts with anionic proteoglycans on the cell surface, resulting in endocytic vesicles [126]. The mechanism of cationic siRNA-lipoplex internalization appears to vary greatly depending on the types of liposomes and/or cells; three studies using different lipoplex formulations have identified macropinocytosis and clathrin-mediated endocytosis for the DLin-MC3-DMA liposomes in HeLa cells and fibroblast NIH3T3 cells, macropinocytosis but not clathrin-mediated endocytosis for the C12-200 liposomes in HeLa cells and other primary cultures of $NPC1^{-/-}$ or $NPC1^{+/+}$ human fibroblast cells, and liposomal fusion with cell membrane but not macropinocytosis and clathrin-mediated endocytosis for the DharmaFECT1 liposomes in 293FT and HeLa cells [91,105,127]. NPC1 is a transmembrane protein that regulates the exocytosis of MVB contents.

Perturbation of the endocytic pathway alters the transport and residence of NP therapeutics. For example, the blocking of the fusion of late endosomes to lysosomes using siRNA against HPS4, a protein required for the fusion, resulted in accumulation of active RISC-siRNA-target mRNA complexes (GW-bodies) and greater siRNA-mediated gene knockdown. In contrast, the down-regulation of ESCRT, resulted in fewer GW-bodies and impaired gene silencing [128]. Cells deficient in NPC1 (which positively regulates MVB fusion with cell membrane and subsequent exosome release) show greater intracellular retention and greater endosomal escape of, and improved gene silencing by, RNAi-lipoplex [105]. These observations suggest lysosomal degradation and exosome release are quantitatively important mechanisms for clearing intracellular siRNA.

Of interest is the recent finding that RISC is physically associated with MVB and that MVB formation affects the loading and unloading of siRNA on RISC [129].

An earlier study shows that the half-life of the siRNA gene silencing, when siRNA is loaded in oligofectamine or polymeric NP, is relatively long, lasting from several days to 3 weeks [130]. However, less is known regarding the kinetics of the individual steps in the siRNA-mediated mRNA degradation, i.e., release of siRNA from endosomes or from its carriers, siRNA binding with and release from RISC, binding of the RISC/siRNA complex with mRNA, and cleavage of mRNA. For example, due to the multiple pathways for internalizing siRNA-carriers, it is not clear whether the cytosolic siRNA derives from the direct release from its carrier after entering cells through fusion or from endosomes after endocytosis, or at which point of the endocytic pathway the siRNA is released. The ambiguity is caused in part by a lack of methodology to reliably visualize the intracellular movement of siRNA, e.g., live cell confocal microscopy cannot distinguish if changes in the fluorescence intensity of the labeled siRNA is due to its release from the endosomes or due to photobleaching or movement in-and-out of the imaging plane. Nonetheless, the current data suggest the siRNA release from endosomes is dependent on the type of lipoplex. For example, a recent study used fluorescently labeled galectin-8 to study the onset of endosomal leakage; this protein monitors endosome integrity and is recruited to damaged endosomes to initiate autophagy.

The results demonstrate that the lipoplex of siRNA and Lipofectamine recruited galectin-8 within 5–15 min of endosomal uptake, suggesting rapid onset of endosomal membrane damage by this lipoplex. However, because the siRNA functionality was not measured, it is not known whether siRNA was released at the time of endosomal membrane damage or after a delay, or whether siRNA was released as free siRNA or as the original lipoplex [131]. This same study also tested a second liposomal carrier, comprising four lipids (lipid L319, distearoylphosphatidylcholine, cholesterol, pegylated 2-dimyristoyl-sn-glycerol methoxypolyethylene glycol). L319 becomes ionized at the acidic pH of early endosomes and interacts with the negatively charged components of endosomal membrane such as phosphatidylserine. In this case, galectin-8 was recruited to endosomes after 1.5–2 h of endosomal uptake. This event coincided with 50% reduction of the siRNA fluorescence in the lipoplex and with the initiation of gene knockdown, and hence suggests the release of siRNA from both its carrier and endosomes. The difference in the timing of galectin-8 recruitment for the two liposomal carriers suggests the choice of carrier determines the timing of endosomal membrane damage and hence the timing of siRNA release into the cytosol. A separate study using electron microscopy demonstrates that gold NP (originally loaded with siRNA) were released from early, moderately acidic endocytic compartments at 1.5–2 h after endocytic uptake, but whether siRNA was released at the same time or earlier is not known [127].

3.6. Approaches to improve intracellular bioavailability

3.6.1. Promoting internalization—Intracellular bioavailability can be enhanced by manipulating one or more of the internalization mechanisms discussed in 3.2. Conjugation of NP to tumor-specific or tumor-selective ligands, such as transferrin, enhances the internalization by receptor-mediated clathrin-dependent endocytosis [132]. Cell penetrating peptides (CPP) are oligocationic compounds with membrane translocation properties, including TAT (transactivator of transcription) family proteins, penetratin, and chimeric peptide transportan [133–138]. CPP, through interactions with glycosamininoglycan, adsorb on cell membrane and induce fusion and macropinocytosis [139–142]. CPP-modified liposomes are also internalized *via* clathrin-coated pits or caveolin-dependent endocytosis [143–145].

Several NP conjugated with ligands targeting antigens or epitopes on tumor cell surface have been evaluated. The targets include noninternalizing epitopes such as CD20 or internalizing receptors such as CD19, transferrin, HER-2, and uPAR. It is generally known that targeting the noninternalizing epitopes, while it enhances the NP attachment to cells, does not enhance the uptake into cells. In contrast, targeting the internalizing receptors results in rapid NP uptake into cells and improved therapeutic efficacy [146,147]. Additional investigations have led to clinical evaluation of several NP that target internalizing cell surface receptors (e.g., MCC-465, MBP-426, ST-53) [148]. The choice of ligand-receptor interaction affects the rate of NP internalization in cells, e.g., folate receptors show rapid internalization rates of up to 3×105 molecules of folic acid per hr [149].

The spacing and density of targeting ligands also affect the NP internalization. Loading of targeting ligands using a PEG spacer enables the ligand to extend beyond the region where

the ligand would have been sterically hindered by the neighboring PEG molecules, and thereby enhances the NP flexibility and interaction with cell surface receptors [149]. With respect to ligand density, while conjugation with high affinity ligands leads to increased binding and cellular uptake, the same benefit can be achieved by using low-affinity ligands at high densities [148]. The effects of spacing and density on biocorona formation are not known but, in view of the emerging importance of biocorona, merit investigations.

3.6.2. Promoting intracellular release from endosomes/lysosomes—As NP cannot directly cross the endosomal membrane, the general strategy is to promote endosomal escape through one or more of the following four mechanisms [5,150]. First, pore formation on endosomal membrane is a balance between membrane tension that enlarges the pore and line tension that closes the pore. Reduction of the line tension by some compounds, e.g., cationic amphiphilic peptides, stabilizes the pore [92]. Second, protonation induces ion and water flow into endosomes, causing endosomal membrane rupture and cargo release. This proton sponge effect is achieved by the use of lipids or chemicals with high buffering capacity and, when protonated, cause the influx of chloride ions and water molecules to induce osmotic swelling (e.g., histidine-rich molecules, polyamidoamine and polyethylenimine polymers). An example is siRNA carriers comprising cationic or ionizable lipids that are protonated and provide the proton sponge effect [151]. Third, use of agents that destabilize the endosomal membrane and promotes the cargo release into the cytosol. These agents include fusogenic proteins, lipids and peptides that (a) disrupt endosomal membrane (e.g., glutamic acid-alanine-leucine-alanine repeats), (b) enhance the fusion of the carrier with endosomal membrane (e.g. virsomes comprising liposomes modified with a CPP fusogenic viral envelope protein; diINF-7), (c) undergo conformational changes in response to pH changes, which then leads to fusion of the carrier with the endosomal membrane (e.g., hemagglutinin) [152–166], (d) dioleoylphosphatidylethanolamine or DOPE that fuses with endosomal membrane, and (e) pH-sensitive lipids that are degraded under the acidic conditions in late endosomes, e.g., citraconyl-DOPE, promote the unpackaging and release of cargo within the endosome [92]. For pegylated NP, PEG-lipids that are cleaved in the acidic environment of endosomes are used to promote fusion between liposomes with endosomal membrane [152,167–170].

4. Part III. Interactions of nanotherapeutics with tumor microenvironment and extracellular matrix

Interactions of NP with components of biological matrices result in the formation of biocorona [171–173]. This research area is gaining momentum; the number of publications containing NP and corona as key words increased from 9 in 2005 to 134 in 2014. Multiple investigations have documented the interactions between a wide variety of NP (e.g., metallic, metal oxide, carbon based, polymer coated, polymeric nanoparticles, quantum dots, liposomes) with various proteins (apolipoprotein, complement protein, prothrombin, vitronectin, immunoglobulin, fibrinogen, serum albumin) [171,174–177].

4.1. Structure of nanoparticle biocorona

Figure 3 shows the multi-layer biocorona. The first layer of high affinity proteins on the NP surface (referred to as hard corona) is covered by a layer of low-affinity proteins (soft corona) [178,179]. Among the several thousand available proteins in human plasma, only a few dozen are present in the hard corona. Equally intriguing is that the proteins in the hard corona are not necessarily the most abundant proteins in plasma or those with the highest affinity for NP [180].

Biocorona formation, mediated by van der Waals forces and electrostatic interactions, occurs rapidly and is completed within minutes [177]. The formation of biocorona on NP causes increases in particle size (e.g., up to 150% for polystyrene or silica NP) and changes in surface charge (e.g., from positive to neutral or slightly negative). As these two parameters are important determinants of NP disposition/transport and interaction with biological targets (e.g., transfection efficiency), biocorona alters the disposition and functionality of NP, especially for gene therapeutics [174].

4.2. Effect of biocorona on nanoparticle disposition

Formation of biocorona affects the *in vivo* NP biodistribution and clearance, in several ways. NP surface modifications, such as IgG, complement family proteins (C1–C9), fibrinogen and lipoproteins, elicit opsonization and cause entrapment/concentration in RES organs (e.g., Kupffer cells in the liver). Biocorona comprising apolipoproteins such as Apo B and Apo E enables transport across the blood brain barrier [176,181–188], whereas binding to albumin prolongs the circulation time [189,190].

Pegylation of NP has at least two effects. First, pegylation generally decreases biocorona formation, enabling NP to avoid recognition and entrapment in RES [191–194]. However, changes in the extent and composition of biocorona induced by pegylation are dependent on the NP size as well as on the pegylation density. For gold NP, increasing the pegylation density reduces biocorona formation and changes its protein composition, whereas decreasing the NP size leads to a highly curved surface that reduces the steric interaction of PEG molecules and allows more proteins to adsorb to the surface [195]. Second, lowering the zeta potential (from 26 to 2.9 mV) reduces the electrostatic interaction with the negatively charged ECM components (e.g., proteoglycans, fibrous proteins) and thereby enhances the transport of polymeric DNA carriers in the brain parenchyma [196].

4.3. Effect of biocorona on functionality of nanoparticle gene therapeutics

For lipoplexes containing DNA or RNA, their surface charges will vary based on the number of nucleotides. This, in turn, is likely to alter the compositions of the corresponding biocoronae. Adding to this complexity are the recent reports suggesting that interaction of proteins with lipid carriers of DNA or RNAi therapeutics affect the functionality of the gene therapeutics in several ways. First, binding of proteins to RNAi lipoplex causes dissociation of RNAi from NP, presumably due to competition for positively-charged binding sites [197]. The dissociated RNAi or DNA, in turn, is rapidly degraded by endonucleases. Second, the formation of fibrinogen-containing biocorona promotes aggregation of lipoplexes due to a reduction in the electrostatic repulsive forces between lipid membranes [175,198]. Third, a

size increase may hinder extravasation and interstitial transport. On the other hand, the larger NP-biocorona complex may utilize the caveolae-mediated endocytosis pathway that favors larger NP (>500 nm) [198], in addition to the more common clathrin-mediated endocytosis pathway used by smaller NP [199] and the cell membrane fusion pathway [91]. This change in the internalization pathway may affect the eventual transfection efficiency.

4.4. Potential role of tumor microenvironment and extracellular matrix on biocorona formation and stability

As shown in Figure 1, NP-biocorona complex is formed in blood due to NP interactions with serum proteins, whereas NP interactions with proteins present in TME and ECM would yield other biocorona complexes. The formation and stability of NP-biocorona complex, due to the reversibility of noncovalent binding, depend on the concentrations and types of proteins available in the biological milieu. For example, *in vitro* experiments show that low serum protein concentrations lead to biocorona consisting of the more abundant low-affinity proteins, whereas at higher serum concentrations, proteins with higher affinities replace the low affinity proteins and become the predominant component in the biocorona [178,200]. In humans, while serum protein level is generally constant between individuals, the serum protein composition varies with age, ethnicity and physiological or disease state (e.g., autoimmune diseases, cancer) [201,202]. The latter may affect biocorona protein composition and stability. The proteins at the local environment also determine the biocorona composition and the subsequent fate of NP. For example, adsorption of surfactant-associated proteins (SP-A and SP-D) present at lung alveoli onto magnetite NP with either more hydrophilic (starch) or hydrophobic (phosphatidylcholine) surface modifications leads to NP uptake by alveolar macrophages; this mechanism applies to NP with diverse composition, including gold nanoparticles, COOH- and NH_2-surface coated quantum dots, and COOH-modified polystyrene beads [203,204]. These findings suggest the biocorona composition rather than the NP materials was the determining factor for recognition and uptake by macrophages.

It has been proposed that the dynamic process of formation and evolution of NP biocorona is dependent on the relative availability of proteins as NP translocate from one biological compartment to another (e.g., from normal tissues such as blood to tumor tissues) [205,206]. However, there is a lack of information on the site-specific composition of NP biocorona (e.g., whether changes in protein compositions at a specific location or tissue alter the NP fate at the site) and on the quantitative relationship between NP biocorona and target site delivery.

4.5. Perspectives

In view of its significant effects on NP disposition and internalization, future studies on the fate and efficacy of NP therapeutics should take the formation and properties of biocoronae into consideration [173,207]. Potential areas of interests are (a) qualitative and quantitative effects of biocorona on the delivery, transport and residence of NP at different spatial locations of a tumor, (b) effects of biocorona on the internalization and functionality of lipoplex, a widely-used carrier of DNA/RNAi gene therapeutics, (c) inter- and intra-tumoral heterogeneity in biocorona compositions (e.g., tumor necrotic center may have different

protein contents compared to the periphery), (d) exchange of biocorona proteins by proteins in TME or ECM, (e) changes in biocorona as function of time and NP concentration to enable the prediction of NP pharmacokinetics and pharmacodynamics, (f) effects of NP composition on biocorona formation and stability, and (g) species differences. Such information is needed to improve *in vitro*-to-*in vivo* and animal-to-human translation.

5. Part IV. Animal-to-human translation of cancer nanotherapeutics

A major challenge in cancer therapy development is translating the findings in animals to humans. A number of cancer NP therapeutics found effective in animal tumor models do not show activity in humans. For example, Doxil and DaunoXome, the respective liposomal preparations of doxorubicin and daunorubicin, show significant efficacy compared to the corresponding free drugs in multiple preclinical tumor models, but only marginal and insignificant survival benefits in patients compared to doxorubicin-based standard therapy [208–210]. There are many possible causes for the limited success in animal-to-human translation, e.g., biological and genetic variances among experimental and clinical tumors. However, as discussed throughout this review, multiple factors affect the NP transport from injection sites to tumor interstitium, the NP attachment on cells and uptake into cells, and the release of NP and its contents from endosomes. In addition, compared to small molecule drugs that can use both diffusive and convective transport, NP, due to its relatively large size, is more dependent on convective transport and therefore more likely to be negatively impacted by the inherently high interstitial fluid pressure in solid tumors. These variables are likely to cause substantial spatial-temporal-dependent variations in NP delivery and residence in tumors. Hence, the significant heterogeneities and differences in the TME/ECM among animal and human tumors, e.g., small and rapidly growing tumors comprising mostly tumor cells in transplanted animal tumors compared to human tumors that are typically larger in size and comprise mixture of stroma and tumor islets, represent another likely cause. For example, the report of the 2014 NCI Cancer Nanotechnology Workshop highlights the interspecies differences in TME and ECM as a major impediment to successful translation of concepts established in preclinical models, e.g., EPR effect, to clinical application [211].

Quantitative systems pharmacology approaches represent a useful means to account for the time- and spatial-dependent effects of various factors on drug delivery, interstitial transport and residence in tumors, and may be used to facilitate the animal-to-human translation of cancer nanotherapeutics. An example is a recent study that used multiscale computational modeling together with experimental data to evaluate whether liposomes can improve the delivery of doxorubicin to mouse and human tumors, in a qualitatively and quantitatively similar manner in both species. The simulated results demonstrate that, due to differences in transvascular flux and drug/liposome deposition among mouse and human tumors, mouse tumors would show generally greater drug levels for the liposomal formulation compared to the free drug whereas human tumors would not show such benefit under multiple conditions [212]. Additional examples of using multiscale modeling to interrogate and quantify the effects of intratumoral heterogeneity on drug delivery are provided in Part VI.

6. Part V. Immune checkpoint therapy

T cell immune checkpoint inhibitors are the newest therapeutics with demonstrated clinical benefits in cancer patients. Therapeutic success of this therapy requires T cells to contact their target tumor cells, as shown by the positive correlation between the ability of immune cells (e.g., $CD8^+$ T cells) to infiltrate tumors and the treatment outcome [213,214]. Hence, the success of immune checkpoint therapy is subjected to the same delivery barriers as discussed for other therapeutics in this review. These challenges are considerable in view of the much larger size of T cells compared to other conventional cancer therapeutics (7 μm vs. nm range) and the fact that there are many steps between T cell activation and its migration to target sites. TME and tumor ECM are known to contribute to at least 6 mechanisms of immune privilege that protect tumor cells from T cell immunity: (a) active exclusion of T cells from passage through capillary walls, (b) trapping T cells in ECM, (c) physically barring the T cells from contacting tumor cells by way of fibroblast-synthesized ECM structures, (d) chemokine expression or modification that suppresses T cell proliferation, (e) selective recruitment of other immune cell types that reduce the effect of cytotoxic T cells, e.g., macrophage reprogramming that blocks T cell recruitment, and (f) fibroblast-mediated production of CXCL12, a protein that coats and makes tumor cells invisible to T cells [215–218].

6.1. T cell immune therapy

T cell immunity to tumor cells is established in several steps. First, cancer specific antigens released from cancer cells are captured by dendritic cells, a type of antigen presenting cells; this step requires an immune-activating form of cell death (e.g., immunogenic or necrotic, but not apoptotic) [215]. Second, these antigen-containing dendritic cells are drained to a lymph node and interact with the resident naïve T cells, i.e., presenting the cancer cell antigen and exchanging co-activating signals, resulting in the formation of activated cytotoxic T cells that are primed to recognize the antigen-presenting tumor cells. Third, the activated T cell infiltrates the tumor, binds to tumor cells and exerts its cytotoxic actions.

Until the last few years, immunotherapy, including cytokines (interferons, interleukins), cell therapy, and dendritic cell-based vaccines, has provided limited benefits in the management of cancer patients [219]. A likely cause is that tumor cells, by the time of diagnosis, have acquired immune privilege or the protective mechanisms to escape from the immune system [215,216].

6.2. T cell immune checkpoint inhibitors

The status of cancer immunotherapy underwent a drastic change due to the discoveries that activation of two immune checkpoints renders T cells in an “exhausted” state characterized by reduced proliferation and activity, and that inhibition of these checkpoints provides significant clinical benefits. Both checkpoints involve the binding of T cell membrane receptors (cytotoxic T-lymphocyte-associated antigen 4 (CTLA4), programmed death-1 (PD-1)) to ligands, but they have distinct roles in regulating immunity with different temporal and spatial expression patterns (Figure 4). In the first checkpoint, T cell activation by dendritic cells in the lymph node causes the upregulation of CTLA4 that binds to the B7

ligand on the dendritic cell surface, which initiates the signaling that negatively regulates the amplitude of activation [219]. In the second checkpoint, the binding of PD-1 to its ligands PD-L1 or PD-L2 negatively regulates the activity of the activated T cells. PD-L1 and PD-L2 are primarily expressed in inflamed tissues, TME, surfaces of tumor cells, immune cells and fibroblasts. Activated T cells also secrete interferon γ which stimulate PD-L1 and PD-L2 expression. Since 2011, FDA has approved in rapid succession several human monoclonal antibodies directed at these two checkpoints, including ipilimumab, an IgG1-κ immunoglobulin of about 148 kDa that binds to CTLA4, nivolumab, an IgG4-κ immunoglobulin of about 146 kDa that binds to PD-1 [220–223], and pembrolizumab, an IgG4-κ immunoglobulin of about 149 kDa [224] that also binds to PD-1. Studies on combining these two types of inhibitors have been initiated, with encouraging early results [221].

Notable accomplishments of this new immune checkpoint inhibition approach are survival extension and durable response. For example, ipilimumab, given as single agent or in combination with glycoprotein 100 peptide vaccine, extended the overall survival of advanced melanoma patients to about 10 months (*vs* 6.4 months in patients without ipilimumab), with durable responses lasting more than 4 years in 20% of patients [221] [225]. Nivolumab prolonged the median survival in metastatic squamous non-small cell lung cancer patients previously treated with platinum-based therapy, compared to docetaxel (from 6.0 to 9.2 months) [222]. Pembrolizumab yielded a 24% response rate, with sustained response of 6 months or longer in at least 8 of 89 patients [221]. Such accomplishments hold promise for making cancer into a chronic disease. In addition, the nature of immune therapy is such that it may provide a means to achieve the long-elusive goal of a cure. Hence, approaches that improve the effectiveness of immune checkpoint inhibitors may yield therapeutic benefits. The following sections outline the processes that control and determine the effectiveness of T cell immune therapy.

6.3. Migration of activated cytotoxic T cells to reach tumor cells

The subjects of leukocyte activation, recruitment, rolling and adhesion on endothelium, transvascular and interstitial migration have been extensively studied. These processes are controlled by a large number of adhesion molecules, receptors, cytokines, chemokines, chemoattractants, signaling pathways, sheer stress due to blood flow, and cell types (e.g., endothelial cells, pericytes). Most of the large body of literature concerns inflammation. There is evidence that some of the regulatory mechanisms may be different in cancer. Readers are directed to several excellent reviews for detailed discussions [215,217,218,226,227]. A brief summary is as follows.

6.3.1. Trafficking of leukocytes to tissues—The original 3-step model of leukocyte rolling, adhesion and transmigration was first described in the nineteenth century; Figure 5A shows an updated model of the adhesion cascade. The four phases are as follows. (a) Rolling of leukocytes on endothelial cells to reach the target tissue involves sequential interactions between homing receptors on leukocytes, selectins, integrins, and their corresponding binding ligands. The specificity of the homing receptors depends on the location of the lymph node in which T cell is activated and on the antigen-presenting dendritic cells. The

expression of vasculature ligands is modified by inflammatory cytokines and other events including radiation. (b) Leukocyte activation and arrest on endothelium is controlled by integrins, chemokines, chemo-attractants, their corresponding binding ligands or receptors (e.g., G-protein coupled receptors) and the subsequent signaling pathways. These processes involve a vast network of at least 900 proteins and at least 6000 protein-protein interactions. It has been shown that the expression of leukocyte homing receptor ligands on tumor vasculature is generally lower compared to surrounding normal tissues [226], which may be a cause of inadequate tumor immunity. (c) Transendothelial migration comprises two different steps (Figure 5B). In the first step of crawling, leukocytes roll inside blood vessel and seek preferred sites for transvascular migration. Disablement of crawling delays the migration. The second step is crossing the endothelium, which occurs *via* paracellular or transcellular routes, with the latter being the minor path. (d) Leukocytes migrate through the endothelial basement membrane and pericyte sheath. The basement membrane is composed of two protein networks comprising laminins and collagen type IV. The low protein expression sites colocalize with gaps between pericytes, representing regions of least resistance. Transendothelial migration is more rapid compared to penetration through the basement membrane (<2–5 *vs.* >5–15 min); these processes are affected by the composition of cell types (endothelial *vs.* pericytes) and basement membrane. In general, disorganized tumor capillaries formed in response to proangiogenic factors reduces transvascular leukocyte migration, and low dose antiangiogenic therapy may enhance immunological tumor control through normalization of tumor vessels.

6.3.2. Migration of leukocytes in tissue interstitium—In contrast to the transendothelial migration that requires adhesion by ligand-homing receptor-dependent mechanisms, leukocyte migration in 3-dimensional interstitial ECM is integrin-independent and is either not or only partially dependent on adhesion. This process, known as contact guidance, is mediated by an actin flow along the confining ECM scaffold structure, shape change, squeezing through available space and following paths of least resistance.

6.3.3. Barriers to T cell migration in tumors—The above processes observed for inflamed and peripheral tissues appear to also occur in tumors. In transplantable murine tumors, adoptively transferred fluorescent T cells first migrate at tumor periphery, conjugate with tumor cells, and then regain motility and progressively infiltrate the tumor center, with T cell migration occurring along collagen fibers or blood vessels [218,228,229].

Several recent studies addressed the barrier roles of ECM in interstitial T cell migration in human tumors [213,218,230–233]. The notable findings are as follows. First, in contrast to transplantable tumors that typically comprise mostly tumor cells, patient tumors show clusters of tumor cells surrounded by stroma containing collagen and fibronectin strands in varying densities, with areas of high collagen density in the immediate proximity of tumor cells. Second, the tumor ECM structures determine the interstitial T cell migration and distribution. Surgical specimens of human tumors show substantial, up to 100-fold intratumoral spatial variation in T cell density, with higher T cell frequencies in the invasive margin compared to the core. Third, in human pancreatic tumors, the distribution of T cells favors the stroma relative to tumor islets, i.e., present at higher frequency in the stroma and

absent from the tumor islets in 70% of samples. In addition, the T cell frequency does not show spatial correlation with the overexpression of several T-cell active chemokines (CXCL12, IP-10, MIP-1β) but instead is spatially correlated with collagen density in an inverse relationship. The latter has been confirmed in fabricated 3-dimensional collagen matrices; maximal migration occurs at the lowest collagen density of 0.5 mg/mL whereas a higher density of 1.5 mg/mL nearly completely abolishes T cell invasion. Fourth, treatment of tumors with collagenase reduces collagen density and enhances T cell infiltration into tumor islets. Fifth, a study of the migration of fluorescently labeled activated T cells in slices of patient lung tumors (over 20 min) using live cell confocal microscopy shows the following: (a) T cells move in parallel with collagen and fibronectin fibers, (b) T cells cannot cross the dense matrix areas characterized by bands of thick and linear collagen fibers running parallel to tumor islets, (c) T cell movement in the favorable migration zones, characterized by a reticular network of thinner fibers similar to the zones of lymph nodes housing high T cell concentrations, is multi-directional and is several-fold more rapid than in the dense collagen fiber zones, and (d) T cells enter tumor islets through the favorable migration zones. The inverse correlation between stromal structure and T cell distribution is in agreement with an earlier finding in rat tumors that T cells are absent in the area of activated fibroblasts surrounding tumor islets [234].

Taken together, the above findings establish the composition, fiber density, organization and architecture of TME and ECM as major barriers and determinants of the interstitial transport of T cells.

6.4. Tumor heterogeneity and specificity: Role of tumor microenvironment and extracellular matrix

Histopathological analyses of a variety of human tumors show highly variable T cell density (e.g., ~100-fold for CD8+ cells) and highly variable distribution in different parts within a tumor. It has been proposed that the variabilities in T cell frequency play a role in patient prognosis [213,235]. Likewise, differences in TME and ECM, as determinants of T cell distribution, may explain the differences in resistance to immune checkpoint therapy between tumors where some tumor types such as pancreatic cancer or prostate cancer are more resistant to the therapy compared to melanoma [236]. Similarly, certain metastatic sites, e.g., visceral metastatic sites (liver, lung, brain), are more resistant to the therapy compared to bone marrow [236].

6.5. Approaches to improve T cell infiltration in tumors

Several approaches focusing on reducing the ECM-mediated transport barriers have been proposed [218,237,238]. These include (a) reduction of ECM density by inhibiting lysyl oxidase that is elevated in human tumors and mediates the cross-linking of collagen fibers, (b) reduction of myofibroblasts that play a key role in the production and remodeling of ECM, (c) reduction of fibroblast activation protein α, (c) reduction of TGF-β, a cytokine associated with myofibroblast activation and ECM/collagen deposition, (d) blocking ECM-induced signaling pathways, e.g., sonic hedgehog and focal adhesion kinase signaling. Other targets being investigated include matrix metalloproteinases, collagenase and hyaluronidase.

7. Part VI. Computational approaches to interrogate and quantify the effects of tumor microenvironment and extracellular matrix

7.1. Use of computational models to capture heterogeneities in tumor properties and therapeutics

As discussed above, tumors are highly heterogeneous and many tumor properties (a) are dynamic and change with time (e.g., size, blood flow, tumor cell density, TME, ECM, vascularization status, growth rate, capillary pore size and permeability, extracellular proteins), (b) depend on the host (e.g., larger tumors in humans than in mice), (c) are patient-dependent (e.g., location in relation to normal tissues, size), (d) can change with time (e.g., tumor growth) or with treatments (e.g., cell death due to chemotherapy or irradiation, altered vasculature due to anti-angiogenics), and (e) are inter-dependent where changes in one property can affect other properties (e.g., increase in tumor size will affect the vascularization) [12]. In addition, interactions between therapeutic and biological matrices in tumors and other organs affect the disposition, transport and residence of the therapeutic in tumors. NP therapeutics, due to their diverse properties (e.g., size, surface modifications, aggregation) present yet another level of complexity. For example, pegylation of NP increases the circulation time but also decreases the endocytosis, and surface charge and pegylation have opposing quantitative effects on NP binding to cell surface and NP internalization such that the effect of one parameter is offset by the other [58]. These diverse and dynamic properties and interactions create uncertainties on the delivery of a therapeutic to its intended target site and accordingly uncertainties on the treatment efficacy.

Our group shares the view that there is a need for developing computational models to capture the above factors and using these models to quantitatively interrogate how changes in these parameters, separately or collectively, affect the delivery and residence of a therapeutic at the target site. Such models represent a potentially useful tool to reduce the empiricism and ambiguities (e.g.,[239,240]). This approach is beginning to take shape, as shown by the increasing number of publications from multiple investigator teams on using computational models to depict drug/NP delivery and transport in the last five years. For example, based on the published results on tumor priming from our group and others (see 2.3.3, another group of investigators established a computational, physiologically-based pharmacokinetic and pharmacodynamic model and used it to simulate the optimal time window for tumor priming [241]. This model takes into account the release of doxorubicin from liposomes and the simulation results indicate that fine-tuning the tumor priming schedule (i.e., using a 24-h interval between paclitaxel priming and liposomal doxorubicin instead of the 48-h interval we selected based on the time course of tumor cellularity changes induced by paclitaxel alone) would further enhance the doxorubicin levels in tumors by 2.5-fold.

7.2. Models for drug/nanoparticle transport

The modeling of interstitial diffusive and/or convective transport of small molecule drugs has been used to describe drug release from delivery systems (e.g., [242,243]). This approach has also been used to improve drug delivery and therapeutic efficacy. One example is the modeling of the distribution of drugs delivered intracranially to the brain [244].

Another example is our development of the apoptosis-inducing tumor-priming concept and the subsequent development of drug-loaded particles with the dual actions of priming and maintenance [12,63–65,245–248]. Modeling the doxorubicin diffusive transport in liver tumors provided the basis for using radiation-ablation therapy to enhance drug dispersion [249]. The above earlier transport models primarily focus on the tumor and do not include transvascular transport or connection to other organs. In comparison, the more recent models include both interstitial and transvascular transport by diffusion and convection, and are often multiscale in nature (e.g., combination of spatial and time scales, combination of microscopic (e.g., molecule or cell) and macroscopic scales (e.g., tissue or whole organism)). The multiscale feature is particularly useful in capturing the spatial- and time-dependent changes and the heterogeneities in tumor properties, as well as for dealing with specific components of interests (e.g., delivery and residence of vessel-targeting NP). These publications are in two general categories. The first category describes the development of theoretical models to capture the known tumor pathobiological parameters and the physical processes underlying the transport processes (e.g., [250–254]). While these publications do not provide experimental verifications of the proposed models, they are excellent resources for model development. The second category, far fewer in numbers, describes models with experimental verifications. An example is the multiscale modeling study described in section 2.3.3 [212]; this study used a model that includes kinetic processes on several scales: (a) systemic disposition/elimination in whole organism, (b) transvascular flux in tumor, and (c) several processes on cellular level (e.g., internalization, binding to DNA, efflux). Distinguishing these processes on different scales enabled the investigators to conclude that the differences in transvascular flux of doxorubicin and liposomal doxorubicin among mouse and human tumors result in qualitative/quantitative differences in the benefit of using liposomal doxorubicin in these species.

Our group has been working on predictive models of drug/NP transport, delivery and residence in solid tumors, under *in vitro* and *in vivo* conditions. To our knowledge, there are only two other studies within the last 5 years where the model-predictions were in good agreement with the experimental results (arbitrarily defined as <100% deviations). The first is an *in vitro* study that used models of NP diffusion and cellular uptake to depict the diffusive transport in 3-dimensional tumor cell cylindroids [255]. The second is an *in vivo* study that used modeling to predict the increase in the delivery of doxorubicin-loaded heat-sensitive liposomes in tumors by hyperthermia; the model successfully predicted the spatial distribution of hyperthermia, intracellular doxorubicin and cell kill [256]. The following sections describe the approaches and findings of our studies [257–260].

7.3. Predictive models of *in vitro* interstitial diffusive transport based on nanoparticle-cell interaction parameters

7.3.1. Hypothesis and experimental systems—We first tested the hypothesis that the interstitial diffusive NP transport can be predicted using (a) NP-cell biointerface parameters (binding, association, dissociation, internalization) measured in monolayer cell cultures, plus (b) NP diffusivity in tumor interstitium calculated based on NP size and interstitial structure and composition [257,258].

The avascular 3-dimensional tumor cell spheroids, devoid of convective transport, were used as the model system. Spheroids are aggregates of tumor cells without blood vessels, retain many properties of solid tumors (e.g., multicellular structures, extracellular matrix, tight junctions between cells, gradients of nutrient and oxygen concentrations and heterogeneous cell proliferation rate), and are considered a surrogate of solid tumors for studying drug delivery and patient tumor sensitivity to specified drugs [10,261–263]. For our purpose, the absence of vasculature in spheroids ascertains that the transport was due to diffusion and not confounded by convection. Experiments were performed with three types of NP, i.e., negatively-charged polystyrene beads, near-neutral zwitterionic liposomes sterically stabilized with pegylation, and pegylated cationic liposomes with fusogenic properties, all fluorescently labeled. These three NP cover a wide range of sizes (20–130 nm) and surface charges (− 49 to +38 mV); their different properties resulted in 3- to 150-fold differences in NP-cell interaction parameters which in turn led to 3-fold differences in their interstitial diffusive transport [257].

7.3.2. Model assumptions and parameterization—The first generation computation models used the assumptions of negligible NP efflux from cells, only unbound NP (i.e., NP not associated with cells) are available for diffusion, equal numbers of binding sites for cells in monolayers and in 3-dimensional structures, absorptive and receptor-mediated NP endocytosis, specific and saturable binding of NP to cell membrane and negligible NP binding to ECM [257,258]. The models accounted for the diffusive flux created by the concentration gradient and the depletion of the unbound NP due to cell binding and internalization. The effect of biocorona was also partially accounted for because the culture medium contained 10% fetal bovine serum. The parameters for NP-cell interactions, because they are dependent on NP properties and cell properties, were experimentally determined using monolayer cultures; these include the rate constants for binding, dissociation and internalization, and the number of binding sites on cell surface. Other model parameters that are independent on NP properties were obtained or calculated from literature data. For example, the interstitial NP diffusivity was calculated based on NP size and TME parameters (i.e., tumor cell density, interstitial void volume fraction, concentrations and diameters ECM proteins/fibers). The equations were solved numerically using the finite element method [258].

7.3.3. Experimental results and evaluation of model performance—The first generation models successfully predicted the interstitial transport of the anionic, near neutral and cationic NP, such that the predicted concentration-depth profiles in spheroids at multiple initial concentrations and treatment durations (3 concentrations and 3 durations for each NP), were within the 95% confidence intervals of experimental data (Figure 6) [257,258]. The only exception was the cationic liposomes containing high fusogenic lipid contents (>10 mol%), presumably due to nonlinear changes in liposome-cell interactions that were not captured in the models [258].

7.3.4. Model-simulations to interrogate the effects of NP properties on interstitial diffusive transport—Results of *in silico* studies using the above models indicate the following.

- Diffusion is slow and rate-limiting for interstitial NP transport.
- Changes in NP surface charge affect the NP distribution in interstitial space and subcellular compartments.
- Delivery and penetration for all three NP in spheroids increase with treatment time, with the greatest increases for the neutral NP (2- to 3-times higher compared to charged NP).
- For anionic and cationic NP, interactions with cells and size increases secondary to biocorona formation, respectively, reduce diffusion by 2- and 30-fold.
- For cationic NP, >98% of the amount in spheroids is represented by the cell surface-bound and internalized NP. These two entities showed different kinetics. The surface-bound amount initially increasing over time (e.g., 6 h) and then remaining relatively constant due to saturation of binding sites. In contrast, the internalized amount continued to increase with time. Accordingly, the differences in the total amount of NP caused by changes in the NP properties (e.g., cationic lipid content and surface charge) at early time points (e.g., first 6 h) was primarily due to their different cell binding capacities, whereas the differences at later times were primarily due to their different extents of internalization.

We propose that predictive NP transport models offer a means to optimize NP design to achieve the desired delivery and retention at the intended target sites (e.g., tumor interstitium for therapeutics that act on extracellular targets, cell membrane for antibodies, or cytosol for RNAi) [258].

7.4. Multiscale models to capture tumor spatial heterogeneities and to predict *in vivo* spatiokinetics of therapeutics

The above models address only the interstitial diffusive transport as functions of NP-cell interactions and interactions with the ECM present in the serum-containing culture medium. Depiction of the disposition of a therapeutic in a host requires the inclusion of several additional models to account for interstitial transport *via* fluid flow-mediated convection, transvascular transport (both into and out of vessels *via* diffusion and convection), interaction with TME in addition to tumor cells (e.g., vessel wall, stromal tissues), and other processes that affect its disposition (e.g., distribution to other organs, elimination). Our group has used multiscale models for this purpose [259]. Multiscale models enable the calculation of certain properties on one level (e.g., solid tumor) based on the information from different levels (e.g., whole organism), with each level addressing a phenomenon over a specific window of length and time. For example, our models connect the drug disposition on three scales (tumor, intraperitoneal cavity, whole organism), with individual models accounting for the distinct processes on a single scale (e.g., spatial-dependent variations in TME/ECM in the tumor-scale model).

7.4.1. Hypothesis and experimental systems—This *in vivo* study tested the hypothesis that multiscale models are useful for predicting the spatial-dependent changes in drug/NP concentrations within a tumor (referred to as spatiokinetics) as functions of other readily measured parameters (drug-cell-ECM interactions, drug disposition in peritoneal

fluid and whole organism) and elapsed time [259]. The test drug was ^{3}H-labeled paclitaxel which is extensively bound to serum protein such as albumin that has a hydrodynamic diameter of 7 nm [264]. Tumor-bearing mice were given an intraperitoneal injection of paclitaxel solubilized in Cremophor and ethanol. Samples of blood and peritoneal fluid were analyzed to establish the concentration-time profiles. Solitary tumors located on the omentum were analyzed for drug concentration-depth profiles.

7.4.2. Model assumptions and parameterizations—For transport, we assumed (a) that fluid exchange between tumors, peritoneal cavity, and incoming blood vessels depend on the pressure gradients in these three compartments, (b) that drug transport in tumor interstitium occurred by diffusion and convection in a porous gel structure, (c) no lymphatic transport in tumors, (d) no time- or spatial-dependent changes in vessel permeability, venous pressure or drug-cell binding parameters, (d) negligible drug binding to ECM in view of the more extensive drug association with cells compared to extracellular macromolecules, and (e) only drug not associated with cells was available for transport. Note that some of these assumptions are valid only for early time points prior to treatment-induced changes in TME occurs (e.g., 6 h).

Figure 7A shows the multiscale models. The peritoneal cavity-scale model accounts for the drug removal from the cavity *via* lymphatic drainage and/or absorption, processes determined by host properties (intraperitoneal pressure, peritoneal fluid volume), and drug properties (molecular size, binding to proteins). The whole organism-scale model accounts for the drug distribution to various organs and the drug clearance from the body (e.g., metabolism, renal excretion). The tumor-scale model (a) accounts for the intratumoral heterogeneities in TME and ECM (e.g., vessel density, tumor cell density, IFP, ECM proteins) as functions of locations within a tumor and thereby accounts for the spatial-dependent interstitial and transvascular drug transport, (b) accounts for the drug properties with respect to drug-cell-TME/ECM interactions, and (c) uses the drug concentration-time profiles in peritoneal fluid and systemic blood as the respective boundary conditions (drug source) at tumor border and tumor blood vessels for calculating the drug concentrations in tumors. Because paclitaxel is extensively bound to cellular and extracellular components, the tumor is viewed as comprising three subcompartments (i.e., cells to which the drug associates, interstitial space/fluid where the drug undergoes interstitial transport, and vessels where the drug undergoes transvascular transport). Integration of the models on the three scales enables the calculation of changes in the concentrations of the respective drug moiety (i.e., cell-associated drug, unbound drug undergoing interstitial transport and unbound drug undergoing transvascular transport) as function of time and spatial positions in a tumor.

As discussed in sections 2.3.3 and 6.1, an earlier multiscale model was successfully used to address the mouse-to-human translatability [212]. This earlier model views the entire tumor as a single compartment. Because our purpose is to examine tumor spatiokinetics as a function of intratumor heterogeneities, our tumor-scale model separated the tumor into segments with known intratumoral heterogeneities, and captured the heterogeneities by including several spatial-dependent model parameters. Another difference is our model accounted for both diffusive and convective transport whereas the earlier model used a single transport process. Briefly, our tumor-scale model used two types of model parameters. The

spatial-independent parameters include parameters for drug transfer across vessel wall and drug-cell interactions, intraperitoneal pressure, and microvascular pressure. The spatial-dependent model parameters that change due to intratumor heterogeneity include the volume fractions of cells, vessels, and interstitial space (less cells and less vessels in the necrotic tumor center), IFP (higher in tumor than in adjacent normal tissue), effective diffusivity and hydraulic conductivity (higher in tumor center than in tumor periphery), and vessel surface area (higher in periphery than in center). The parameters that are drug- and cell-specific were measured experimentally and the remainders were calculated or obtained from the literature.

7.4.3. Experimental results and evaluation of model performance—Figure 7B shows the experimental results on the drug disposition on three scales. The drug concentration-time profiles in the peritoneal fluid and plasma describe the drug disposition in the peritoneal cavity-scale and the whole organism-scale, respectively, whereas the drug concentration-depth profiles in the tumors resected from four mice describe the spatiokinetics on the tumor-scale. The latter show substantial intertumoral and intratumoral variations. Spatially, the highest drug concentrations were observed at the tumor periphery followed by a sharp decline with increasing distance.

Comparison of the experimentally determined tumor spatiokinetics with the model-predicted profiles indicate good agreement, with deviations that are 60-fold lower compared to the inter-tumor variation among animals (Figure 7C).

7.4.4. Model-simulations to interrogate the effects of intratumoral heterogeneities on spatiokinetics—Results of *in silico* studies show that the time-dependent changes in drug concentrations in peritoneal fluid, tumor interstitium and plasma, plus the nonlinearity and slow rate of drug binding to cells led to substantial, spatial- and time-dependent, and often opposing changes in the interstitial and transvascular drug transport into and out of tumors. Some of the notable findings are as follows.

- The interstitial convective and diffusive drug fluxes are highly time-dependent, decreasing by about 12-fold from 30 min to 6 h. In contrast, the transvascular flux first increases with time to reach a peak at about 20 min and then decline by about 6-fold at 6 h.
- At early time points, the transvascular diffusive interstitium-to-vessel drug flux exceeds the transvascular blood-to-interstitium convective drug flux by 2–3 orders of magnitude.
- Over the first 6 h, (a) the net interstitial flux is in the tumor periphery-to-center direction whereas the net transvascular flux is in the tumor interstitium-to-vessel direction, (b) the net flux from peritoneal cavity into the tumor is the highest initially and diminishes over time; this, coupled with the increasing transvascular flux, results in an outward net flux after 4 h, (c) transvascular diffusive transport has a greater effect compared to the convective transport for removing the drug from tumor interstitium.

- Spatially, while the drug concentrations generally decline with increasing distance from the tumor border, the directions of concentration changes (i.e., increase or decrease) vary with time and spatial positions, and are different for the unbound and cell-bound drug (with greater differences at deeper positions and later times). Changes in drug-cell binding or dissociation parameters result in similar changes in drug flux as changes in convective transport parameters, whereas changes in the maximal cellular binding sites lead to much greater changes. The major drug moiety is the bound drug, especially at deeper parts of the tumor. These data indicate the drug-cell interaction parameters as important determinants of drug delivery to tumors.
- Combined use of the multiscale tumor spatiokinetic models together with the literature *ex vivo* pharmacodynamic data in cultured tumors indicates that during intraperitoneal therapy, only the outermost regions (<1 mm) receives pharmacologically active drug levels. This finding suggests insufficient drug delivery is a major reason that intraperitoneal paclitaxel therapy is ineffective in patients with bulky tumors (i.e., >10 mm) [265].

To our knowledge, the above is the first experimentally verified *in vivo* multiscale tumor spatiokinetics model. This computational tool enables the prediction of the amount/concentration of a drug at the intended target sites (e.g., interstitial fluid, cell membrane-bound, intracellular) based on the numerical values of model parameters that are readily measured *in vitro* or *ex vivo* (e.g., drug-cell-protein interactions measured in cultured tumor cells) or *in vivo* (e.g., pharmacokinetics in blood or other sampling compartments). The *in silico* results further provide potentially clinical useful insights that could not be obtained experimentally, e.g., the finding that transvascular diffusive transport is the major determinant of drug removal from tumor interstitium suggests approaches to reduce such transport may enhance drug residence in tumors. We propose computational multiscale models are useful tools to interrogate the effects of anticipated changes in the diverse and dynamic tumor properties and drug/NP properties, separately or collectively, on the delivery and residence of cancer therapeutics.

8. Part VII. Perspectives

As discussed throughout this review, TME and ECM play important roles in the transport/delivery of a wide variety of cancer therapeutics, including the conventional small molecule drugs, macromolecules, NP, and activated cytotoxic T cells. Manipulation of TME and ECM, through biological or physical means, has emerged as an important research area for cancer translational research. On the other hand, many of the therapeutic-TME/ECM interactions are inter-dependent, are often nonlinear with respect to time and concentration, and, due to intratumoral heterogeneities in TME/ECM, are also spatially dependent. This large number of unavoidable variables leads to many unanswered questions important for patient management. For example, to what extent do treatment-induced changes in vasculature and vessel pore size improve drug delivery? How should one select treatments (dose intensity and dosing interval) in anticipation of intratumoral heterogeneity in the transport mechanisms (diffusion *vs.* convection) in different parts of a tumor? A new trend in cancer combination therapy is adding anti-angiogenic therapy to other standards-of-care.

The dual and time-dependent effects of anti-angiogenic therapy, with initial destruction of less mature vessels and stabilization of other vessels (resulting in temporary increases in tumor blood flow) followed by reduction in blood flow (due to reduced vessel wall permeability and vessel conductivity, reduced vessel density and surface area, reduced vessel radius and pore size) [266–268], are likely to affect drug/NP delivery and retention in tumors. What are the margins of error if the treatment design/selection does not take into account these dynamic processes?

Similarly, while the arrival of nanotechnology presents many new opportunities, there are substantial uncertainties regarding optimal NP properties. For example, increase in tumor size may retard vascularization and NP delivery whereas treatment-induced changes in vasculature and vessel pore size may favor extravasation of larger NP [258]. Larger NP with sizes between the capillary pore size in normal tissues (<10 nm in most tissues) and the pore size in tumor vasculature (typically between 100–200 nm) provides passive tumor targeting, but the larger size retards interstitial transport. NP are frequently surface-modified with targeting ligands to improve targeting and internalization, but binding to cell surface receptors limits NP transport. Pegylation increases circulation times but also decreases the endocytosis of NP [10], and cationic surface charge and pegylation have opposing quantitative effects on NP binding to cell surface and internalization such that the effect of one parameter is offset by the other [58].

In summary, the interactions between a cancer therapeutic (molecules, NP, immune cell), TME, and ECM, are complex and their net effects on the spatiokinetics of the therapeutic are largely unknown. In addition, the pharmacodynamics of cancer therapeutics, due to the drug action mechanisms (e.g., cell cycle specific agents are active against cycling cells whereas only a fraction of tumor cells are proliferating) and the inevitable chemoresistance, is also subjected to uncertainties. These various issues represent interesting and potentially fruitful research opportunities. We advocate using quantitative systems pharmacology approaches, such as those described in Part VI, to address the dynamic interactions, the intratumoral heterogeneities, and the unavoidable time-dependent and patient-dependent changes in tumor properties. Having the ability to predict the target site pharmacokinetics based on the properties of a drug delivery system (e.g., drug release rate or interactions with TME/ECM components) will be a major and useful step to improving the success of its development.

Acknowledgments

This work is supported in part by research grants, R01CA158300, R01CA163015, R43/R44CA103133, R43/R44CA107743, R43CA162448, R01EB015253, R01GM100487, and R43TR000356, from the National Cancer Institute, National Institute of Biomedical imaging and Bioengineering, National Institute of General Medical Sciences, and National Center for Advancing Translational Sciences, NIH, DHHS.

Abbreviations used

Ago-2	argonaute 2
CDE	clathrin-dependent endocytosis

CIE	clathrin-independent endocytosis
CPP	cell penetrating peptides
CTLA4	cytotoxic T-lymphocyte-associated antigen 4
ECM	extracellular matrix
EPR	enhanced permeability and retention
ERC	endosome recycling compartment
ILV	intraluminal vesicle
MVB	multivesicular bodies
NP	nanoparticles
PD1	cytotoxic T cell programmed death-1 membrane receptor
PDL1 and PDL2	PD1 ligands
RES	reticuloendothelial system
RISC	RNA induced silencing complex
RNAi	RNA interference
siRNA	short interfering RNA
TME	tumor microenvironment

References

1. Wei, Y.; Au, JL. Role of tumour microenvironment in chemoresistance. In: Meadows, GG., editor. Cancer Growth and Progression. The Netherlands: Springer; 2005. p. 285-321.
2. Ferrari M. Cancer nanotechnology: opportunities and challenges. Nat. Rev. Cancer. 2005; 5:161–171. [PubMed: 15738981]
3. Kobayashi S, Nakase I, Kawabata N, Yu HH, Pujals S, Imanishi M, Giralt E, Futaki S. Cytosolic targeting of macromolecules using a ph-dependent fusogenic peptide in combination with cationic liposomes. Bioconjug. Chem. 2009; 20:953–959. [PubMed: 19388672]
4. Obata Y, Tajima S, Takeoka S. Evaluation of pH-responsive liposomes containing amino acid-based zwitterionic lipids for improving intracellular drug delivery in vitro and in vivo. J. Control Release. 2010; 142:267–276. [PubMed: 19861141]
5. Li Y, Wang J, Wientjes MG, Au JL. Delivery of nanomedicines to extracellular and intracellular compartments of a solid tumor. Adv. Drug Deliv. Rev. 2012; 64:29–39. [PubMed: 21569804]
6. Wagstaff KM, Jans DA. Nuclear drug delivery to target tumour cells. Eur. J. Pharmacol. 2009; 625:174–180. [PubMed: 19836384]
7. Park TG, Jeong JH, Kim SW. Current status of polymeric gene delivery systems. Adv. Drug Deliv. Rev. 2006; 58:467–486. [PubMed: 16781003]
8. Wang X, Yang L, Chen ZG, Shin DM. Application of nanotechnology in cancer therapy and imaging. CA Cancer J. Clin. 2008; 58:97–110. [PubMed: 18227410]
9. Au JL, Jang SH, Wientjes MG. Clinical aspects of drug delivery to tumors. J. Control. Release. 2002; 78:81–95. [PubMed: 11772451]
10. Jang SH, Wientjes MG, Lu D, Au JL. Drug delivery and transport to solid tumors. Pharm. Res. 2003; 20:1337–1350. [PubMed: 14567626]

11. Wang J, Lu Z, Wientjes MG, Au JL. Delivery of siRNA Therapeutics: Barriers and Carriers. AAPS J. 2010; 12:492–503. [PubMed: 20544328]
12. Wang J, Lu Z, Gao Y, Wientjes MG, Au JL. Improving delivery and efficacy of nanomedicines in solid tumors: role of tumor priming. Nanomedicine. (Lond). 2011; 6:1605–1620. [PubMed: 22077464]
13. Li J, Wientjes MG, Au JL. Pancreatic cancer: pathobiology, treatment options, and drug delivery. AAPS J. 2010; 12:223–232. [PubMed: 20198462]
14. Au JL, Jang SH, Zheng J, Chen CT, Song S, Hu L, Wientjes MG. Determinants of drug delivery and transport to solid tumors. J. Control. Release. 2001; 74:31–46. [PubMed: 11489481]
15. Drummond DC, Meyer O, Hong K, Kirpotin DB, Papahakjopoulos D. Optimizing liposomes for delivery of chemotherapeutic agents to solid tumors. Pharmacol. Rev. 1999; 51:691–743. [PubMed: 10581328]
16. Jain RK. Transport phenomena in tumors. Adv. Chem. Eng. 1994; 19:129–200.
17. Jain RK. Delivery of molecular medicine to solid tumors. Science. 1996; 271:1079–1080. [PubMed: 8599082]
18. Chauhan VP, Lanning RM, Diop-Frimpong B, Mok W, Brown EB, Padera TP, Boucher Y, Jain RK. Multiscale measurements distinguish cellular and interstitial hindrances to diffusion in vivo. Biophys. J. 2009; 97:330–336. [PubMed: 19580771]
19. Eikenes L, Bruland OS, Brekken C, Davies CDL. Collagenase increases the transcapillary pressure gradient and improves the uptake and distribution of monoclonal antibodies in human osteosarcoma xenografts. Cancer Res. 2004; 64:4768–4773. [PubMed: 15256445]
20. Eikenes L, Tari M, Tufto I, Bruland OS, Davies CD. Hyaluronidase induces a transcapillary pressure gradient and improves the distribution and uptake of liposomal doxorubicin (Caelyx (TM)) in human osteosarcoma xenografts. Br. J. Cancer. 2005; 93:81–88. [PubMed: 15942637]
21. Eikenes L, Tufto I, Schnell EA, Bjorkoy A, Davies CD. Effect of Collagenase and Hyaluronidase on Free and Anomalous Diffusion in Multicellular Spheroids and Xenografts. Anticancer Res. 2010; 30:359–368. [PubMed: 20332440]
22. Erikson A, Tufto I, Bjonnum AB, Bruland OS, Davies CD. The Impact of Enzymatic Degradation on the Uptake of Differently Sized Therapeutic Molecules. Anticancer Res. 2008; 28:3557–3566. [PubMed: 19189635]
23. Juweid M, Neumann R, Paik C, Perezbacete MJ, Sato J, Vanosdol W, Weinstein JN. Micropharmacology of Monoclonal-Antibodies in Solid Tumors - Direct Experimental-Evidence for A Binding-Site Barrier. Cancer Res. 1992; 52:5144–5153. [PubMed: 1327501]
24. Suzuki M, Hori K, Abe I, Saito S, Sato H. A new approach to cancer chemotherapy: selective enhancement of tumor blood flow with angiotensin II. J. Natl. Cancer Inst. 1981; 67:663–669. [PubMed: 6944536]
25. Sato H, Urushiyama M, Sugiyama K, Ishizuka K, Hoshi M, Wakui A. Dose intensity and clinical response in patients with advanced gastric carcinoma treated by induced hypertension chemotherapy. Gan To Kagaku Ryoho. 1990; 17:564–569. [PubMed: 2321982]
26. Sato H, Wakui A, Hoshi M, Kurihara M, Yokoyama M, Shimizu H. Randomized controlled trial of induced hypertension chemotherapy (IHC) using angiotensin II human (TY-10721) in advanced gastric carcinoma (TY-10721 IHC Study Group Report). Gan To Kagaku Ryoho. 1991; 18:451–460. [PubMed: 1900686]
27. Nakamura M, Takahashi T, Sato H, Hoshi M, Wakui A, Kanamaru R. Histopathological evaluation on the effect of induced hypertension chemotherapy presurgically performed in patients with advanced carcinoma of the stomach. Tohoku J. Exp. Med. 1992; 167:27–37. [PubMed: 1455418]
28. Abe I, Hori K, Saito S, Tanda S, Li YL, Suzuki M. Increased intratumor concentration of fluorescein-isothiocyanatelabeled neocarzinostatin in rats under angiotensin-induced hypertension. Jpn. J. Cancer Res. 1988; 79:874–879. [PubMed: 2971639]
29. Kalra AV, Campbell RB. Development of 5-FU and doxorubicin-loaded cationic liposomes against human pancreatic cancer: Implications for tumor vascular targeting. Pharm. Res. 2006; 23:2809–2817. [PubMed: 17066329]

30. Bode C, Trojan L, Weiss C, Kraenzlin B, Michaelis U, Teifel M, Alken P, Michel MS. Paclitaxel encapsulated in cationic liposomes: A new option for neovascular targeting for the treatment of prostate cancer. Oncol. Rep. 2009; 22:321–326. [PubMed: 19578772]

31. Ko YT, Falcao C, Torchilin VP. Cationic Liposomes Loaded with Proapoptotic Peptide D-(KLAKLAK)(2) and Bcl-2 Antisense Oligodeoxynucleotide G3139 for Enhanced Anticancer Therapy. Mol. Pharm. 2009; 6:971–977. [PubMed: 19317442]

32. Thurston G, McLean JW, Rizen M, Baluk P, Haskell A, Murphy TJ, Hanahan D, McDonald DM. Cationic liposomes target angiogenic endothelial cells in tumors and chronic inflammation in mice. J. Clin. Invest. 1998; 101:1401–1413. [PubMed: 9525983]

33. Wu J, Lee A, Lu YH, Lee RJ. Vascular targeting of doxorubicin using cationic liposomes. Int. J. Pharm. 2007; 337:329–335. [PubMed: 17275230]

34. Hynes RO. A reevaluation of integrins as regulators of angiogenesis. Nat. Med. 2002; 8:918–921. [PubMed: 12205444]

35. Schottelius M, Laufer B, Kessler H, Wester HJ. Ligands for mapping alphavbeta3-integrin expression in vivo. Acc. Chem. Res. 2009; 42:969–980. [PubMed: 19489579]

36. Ansiaux R, Baudelet C, Jordan BF, Crokart N, Martinive P, DeWever J, Gregoire V, Feron O, Gallez B. Mechanism of reoxygenation after antiangiogenic therapy using SU5416 and its importance for guiding combined antitumor therapy. Cancer Res. 2006; 66:9698–9704. [PubMed: 17018628]

37. Jain RK. Normalization of tumor vasculature: an emerging concept in antiangiogenic therapy. Science. 2005; 307:58–62. [PubMed: 15637262]

38. Tong RT, Boucher Y, Kozin SV, Winkler F, Hicklin DJ, Jain RK. Vascular normalization by vascular endothelial growth factor receptor 2 blockade induces a pressure gradient across the vasculature and improves drug penetration in tumors. Cancer Res. 2004; 64:3731–3736. [PubMed: 15172975]

39. Dickson PV, Hamner JB, Sims TL, Fraga CH, Ng CY, Rajasekeran S, Hagedorn NL, McCarville MB, Stewart CF, Davidoff AM. Bevacizumab-induced transient remodeling of the vasculature in neuroblastoma xenografts results in improved delivery and efficacy of systemically administered chemotherapy. Clin. Cancer Res. 2007; 13:3942–3950. [PubMed: 17606728]

40. Maeda H, Noguchi Y, Sato K, Akaike T. Enhanced vascular permeability in solid tumor is mediated by nitric oxide and inhibited by both new nitric oxide scavenger and nitric oxide synthase inhibitor. Jpn. J. Cancer Res. 1994; 85:331–334. [PubMed: 7515384]

41. Seki T, Fang J, Maeda H. Enhanced delivery of macromolecular antitumor drugs to tumors by nitroglycerin application. Cancer Sci. 2009; 100:2426–2430. [PubMed: 19793083]

42. Yasuda H, Nakayama K, Watanabe M, Suzuki S, Fuji H, Okinaga S, Kanda A, Zayasu K, Sasaki T, Asada M, Suzuki T, Yoshida M, Yamanda S, Inoue D, Kaneta T, Kondo T, Takai Y, Sasaki H, Yanagihara K, Yamaya M. Nitroglycerin treatment may enhance chemosensitivity to docetaxel and carboplatin in patients with lung adenocarcinoma. Clin Cancer Res. 2006; 12:6748–6757. [PubMed: 17121895]

43. Yasuda H, Yamaya M, Nakayama K, Sasaki T, Ebihara S, Kanda A, Asada M, Inoue D, Suzuki T, Okazaki T, Takahashi H, Yoshida M, Kaneta T, Ishizawa K, Yamanda S, Tomita N, Yamasaki M, Kikuchi A, Kubo H, Sasaki H. Randomized phase II trial comparing nitroglycerin plus vinorelbine and cisplatin with vinorelbine and cisplatin alone in previously untreated stage IIIB/IV non-small-cell lung cancer. J. Clin Oncol. 2006; 24:688–694. [PubMed: 16446342]

44. Maeda H. Vascular permeability in cancer and infection as related to macromolecular drug delivery, with emphasis on the EPR effect for tumor-selective drug targeting. Proc. Jpn. Acad. Ser. B Phys. Biol. Sci. 2012; 88:53–71.

45. Maeda H, Nakamura H, Fang J. The EPR effect for macromolecular drug delivery to solid tumors: Improvement of tumor uptake, lowering of systemic toxicity, and distinct tumor imaging in vivo. Adv. Drug Deliv. Rev. 2013; 65:71–79. [PubMed: 23088862]

46. Azzopardi EA, Ferguson EL, Thomas DW. The enhanced permeability retention effect: a new paradigm for drug targeting in infection. J. Antimicrob. Chemother. 2013; 68:257–274. [PubMed: 23054997]

47. Iyer AK, Khaled G, Fang J, Maeda H. Exploiting the enhanced permeability and retention effect for tumor targeting. Drug Discov. Today. 2006; 11:812–818. [PubMed: 16935749]
48. Maeda H, Wu J, Sawa T, Matsumura Y, Hori K. Tumor vascular permeability and the EPR effect in macromolecular therapeutics: a review. J. Control. Release. 2000; 65:271–284. [PubMed: 10699287]
49. Hobbs SK, Monsky WL, Yuan F, Roberts WG, Griffith L, Torchilin VP, Jain RK. Regulation of transport pathways in tumor vessels: role of tumor type and microenvironment. Proc. Natl. Acad. Sci. USA. 1998; 95:4607–4612. [PubMed: 9539785]
50. Moghimi SM, Patel HM. Serum factors that regulate phagocytosis of liposomes by Kupffer cells. Biochem. Soc Trans. 1993; 21:128S. [PubMed: 8359384]
51. Moghimi SM, Davis SS. Innovations in avoiding particle clearance from blood by Kupffer cells: cause for reflection. Crit Rev. Ther. Drug Carrier Syst. 1994; 11:31–59. [PubMed: 7704918]
52. Allen TM, Cullis PR. Liposomal drug delivery systems: from concept to clinical applications. Adv. Drug Deliv. Rev. 2013; 65:36–48. [PubMed: 23036225]
53. He C, Hu Y, Yin L, Tang C, Yin C. Effects of particle size and surface charge on cellular uptake and biodistribution of polymeric nanoparticles. Biomaterials. 2010; 31:3657–3666. [PubMed: 20138662]
54. Elsabahy M, Wooley KL. Design of polymeric nanoparticles for biomedical delivery applications. Chem. Soc. Rev. 2012; 41:2545–2561. [PubMed: 22334259]
55. Illum L, Davis SS. The organ uptake of intravenously administered colloidal particles can be altered using a non-ionic surfactant (Poloxamer 338). FEBS Lett. 1984; 167:79–82. [PubMed: 6698206]
56. Illum SL, Davis SS. Effect of the nonionic surfactant poloxamer 338 on the fate and deposition of polystyrene microspheres following intravenous administration. J. Pharm. Sci. 1983; 72:1086–1089. [PubMed: 6631702]
57. Norman ME, Williams P, Illum L. Influence of block copolymers on the adsorption of plasma proteins to microspheres. Biomaterials. 1993; 14:193–202. [PubMed: 8476992]
58. Li Y, Wang J, Gao Y, Zhu J, Wientjes MG, Au JL. Relationships between liposome properties, cell membrane binding, intracellular processing, and intracellular bioavailability. AAPS. J. 2011; 13:585–597. [PubMed: 21904966]
59. Morrissey DV, Lockridge JA, Shaw L, Blanchard K, Jensen K, Breen W, Hartsough K, Machemer L, Radka S, Jadhav V, Vaish N, Zinnen S, Vargeese C, Bowman K, Shaffer CS, Jeffs LB, Judge A, MacLachlan I, Polisky B. Potent and persistent in vivo anti-HBV activity of chemically modified siRNAs. Nat. Biotechnol. 2005; 23:1002–1007. [PubMed: 16041363]
60. Soutschek J, Akinc A, Bramlage B, Charisse K, Constien R, Donoghue M, Elbashir S, Geick A, Hadwiger P, Harborth J, John M, Kesavan V, Lavine G, Pandey RK, Racie T, Rajeev KG, Rohl I, Toudjarska I, Wang G, Wuschko S, Bumcrot D, Koteliansky V, Limmer S, Manoharan M, Vornlocher HP. Therapeutic silencing of an endogenous gene by systemic administration of modified siRNAs. Nature. 2004; 432:173–178. [PubMed: 15538359]
61. Kuh HJ, Jang SH, Wientjes MG, Weaver JR, Au JL. Determinants of paclitaxel penetration and accumulation in human solid tumor. J. Pharmacol. Exp. Ther. 1999; 290:871–880. [PubMed: 10411604]
62. Griffon-Etienne G, Boucher Y, Brekken C, Suit Hd, Jain RK. Taxane-induced apoptosis decompresses blood vessels and lowers interstitial fluid pressure in solid tumors: clinical implications. Cancer Res. 1999; 59:3776–3782. [PubMed: 10446995]
63. Jang SH, Wientjes MG, Au JL. Enhancement of paclitaxel delivery to solid tumors by apoptosis-inducing pretreatment: effect of treatment schedule. J. Pharmacol. Exp. Ther. 2001; 296:1035–1042. [PubMed: 11181938]
64. Lu D, Wientjes MG, Lu Z, Au JL. Tumor priming enhances delivery and efficacy of nanomedicines. J. Pharmacol. Exp. Ther. 2007; 322:80–88. [PubMed: 17420296]
65. Wang J, Lu Z, Yeung BZ, Wientjes MG, Cole DJ, Au JL. Tumor priming enhances siRNA delivery and transfection in intraperitoneal tumors. J. Control Release. 2014; 178:79–85. [PubMed: 24462901]

66. Cui M, Au JL, Wientjes MG, O'Donnell MA, Loughlin KR, Lu Z. Intravenous siRNA silencing of survivin enhances activity of mitomycin C in human bladder RT4 xenografts. J. Urol. 2015; 194:230–237. [PubMed: 25681288]

67. Nagano S, Perentes JY, Jain RK, Boucher Y. Cancer cell death enhances the penetration and efficacy of oncolytic herpes simplex virus in tumors. Cancer Res. 2008; 68:3795–3802. [PubMed: 18483263]

68. Cho H, Kwon GS. Polymeric micelles for neoadjuvant cancer therapy and tumor-primed optical imaging. ACS Nano. 2011; 5:8721–8729. [PubMed: 21999531]

69. Hylander BL, Sen A, Beachy SH, Pitoniak R, Ullas S, Gibbs JF, Qiu J, Prey JD, Fetterly GJ, Repasky EA. Tumor Priming by Apo2L/TRAIL Reduces Interstitial Fluid Pressure and Enhances Efficacy of Liposomal Gemcitabine in a Patient Derived Xenograft Tumor Model. J. Control Release. 2015; 217:160–169. [PubMed: 26342663]

70. Geretti E, Leonard SC, Dumont N, Lee H, Zheng J, De SR, Gaddy DF, Espelin CW, Jaffray DA, Moyo V, Nielsen UB, Wickham TJ, Hendriks BS. Cyclophosphamide-Mediated Tumor Priming for Enhanced Delivery and Antitumor Activity of HER2-Targeted Liposomal Doxorubicin (MM-302). Mol. Cancer Ther. 2015; 14:2060–2071. [PubMed: 26162690]

71. Shi W, Wang J, Fan X, Gao H. Size and shape effects on diffusion and absorption of colloidal particles near a partially absorbing sphere: implications for uptake of nanoparticles in animal cells. Phys. Rev. E. Stat. Nonlin. Soft. Matter Phys. 2008; 78:061914. [PubMed: 19256875]

72. Israelachvili JN, Wennerstrom H. Entropic Forces Between Amphiphilic Surfaces in Liquids. J. Phys. Chem. 1992; 96:520–531.

73. Chandler D. Interfaces and the driving force of hydrophobic assembly. Nature. 2005; 437:640–647. [PubMed: 16193038]

74. Du H, Chandaroy P, Hui SW. Grafted poly-(ethylene glycol) on lipid surfaces inhibits protein adsorption and cell adhesion. Biochim. Biophys. Acta. 1997; 1326:236–248. [PubMed: 9218554]

75. Peer D, Karp JM, Hong S, Farokhzad OC, Margalit R, Langer R. Nanocarriers as an emerging platform for cancer therapy. Nat. Nanotechnol. 2007; 2:751–760. [PubMed: 18654426]

76. Matsudaira H, Asakura T, Aoki K, Searashi Y, Matsuura T, Nakajima H, Tajiri H, Ohkawa K. Target chemotherapy of anti-CD147 antibody-labeled liposome encapsulated GSH-DXR conjugate on CD147 highly expressed carcinoma cells. Int. J. Oncol. 2010; 36:77–83. [PubMed: 19956835]

77. Yang T, Choi MK, Cui FD, Kim JS, Chung SJ, Shim CK, Kim DD. Preparation and evaluation of paclitaxel-loaded PEGylated immunoliposome. J. Control. Release. 2007; 120:169–177. [PubMed: 17586082]

78. Lukyanov AN, Elbayoumi TA, Chakilam AR, Torchilin VP. Tumor-targeted liposomes: doxorubicin-loaded long-circulating liposomes modified with anti-cancer antibody. J. Control. Release. 2004; 100:135–144. [PubMed: 15491817]

79. Mamot C, Drummond DC, Greiser U, Hong K, Kirpotin DB, Marks JD, Park JW. Epidermal growth factor receptor (EGFR)-targeted immunoliposomes mediate specific and efficient drug delivery to EGFR- and EGFRvIII-overexpressing tumor cells. Cancer Res. 2003; 63:3154–3161. [PubMed: 12810643]

80. Xiang GY, Wu J, Lu YH, Liu ZL, Lee RJ. Synthesis and evaluation of a novel ligand for folate-mediated targeting liposomes. Int. J. Pharm. 2008; 356:29–36. [PubMed: 18258394]

81. Hatakeyama H, Akita H, Maruyama K, Suhara T, Harashima H. Factors governing the in vivo tissue uptake of transferrin-coupled polyethylene glycol liposomes in vivo. Int. J. Pharm. 2004; 281:25–33. [PubMed: 15288340]

82. Eavarone DA, Yu XJ, Bellamkonda RV. Targeted drug delivery to C6 glioma by transferrin-coupled liposomes. J. Biomed. Mater. Res. 2000; 51:10–14. [PubMed: 10813739]

83. Khalil IA, Kogure K, Akita H, Harashima H. Uptake pathways and subsequent intracellular trafficking in nonviral gene delivery. Pharmacol. Rev. 2006; 58:32–45. [PubMed: 16507881]

84. Huotari J, Helenius A. Endosome maturation. EMBO J. 2011; 30:3481–3500. [PubMed: 21878991]

85. Mathivanan S, Ji H, Simpson RJ. Exosomes: extracellular organelles important in intercellular communication. J. Proteomics. 2010; 73:1907–1920. [PubMed: 20601276]

86. McMahon HT, Boucrot E. Molecular mechanism and physiological functions of clathrin-mediated endocytosis. Nat. Rev. Mol. Cell Biol. 2011; 12:517–533. [PubMed: 21779028]

87. Rejman J, Oberle V, Zuhorn IS, Hoekstra D. Size-dependent internalization of particles via the pathways of clathrin- and caveolae-mediated endocytosis. Biochem. J. 2004; 377:159–169. [PubMed: 14505488]

88. Parton RG. Caveolae meet endosomes: a stable relationship? Dev. Cell. 2004; 7:458–460. [PubMed: 15469832]

89. Doherty GJ, McMahon HT. Mechanisms of Endocytosis. Annu. Rev. Biochem. 2009; 78:857–902. [PubMed: 19317650]

90. Mercer J, Helenius A. Virus entry by macropinocytosis. Nat. Cell Biol. 2009; 11:510–520. [PubMed: 19404330]

91. Lu JJ, Langer R, Chen J. A novel mechanism is involved in cationic lipid-mediated functional siRNA delivery. Mol. Pharm. 2009; 6:763–771. [PubMed: 19292453]

92. Schroeder A, Levins CG, Cortez C, Langer R, Anderson DG. Lipid-based nanotherapeutics for siRNA delivery. J. Intern. Med. 2010; 267:9–21. [PubMed: 20059641]

93. Scita G, Di Fiore PP. The endocytic matrix. Nature. 2010; 463:464–473. [PubMed: 20110990]

94. Boettner DR, Chi RJ, Lemmon SK. Lessons from yeast for clathrin-mediated endocytosis. Nat. Cell Biol. 2012; 14:2–10. [PubMed: 22193158]

95. Anitei M, Hoflack B. Bridging membrane and cytoskeleton dynamics in the secretory and endocytic pathways. Nat. Cell Biol. 2012; 14:11–19. [PubMed: 22193159]

96. Rusten TE, Vaccari T, Stenmark H. Shaping development with ESCRTs. Nat. Cell Biol. 2012; 14:38–45. [PubMed: 22193162]

97. Vaughan EE, Dean DA. Intracellular trafficking of plasmids during transfection is mediated by microtubules. Mol. Ther. 2006; 13:422–428. [PubMed: 16301002]

98. Coppola S, Cardarelli F, Pozzi D, Estrada LC, Digman MA, Gratton E, Bifone A, Marianecci C, Caracciolo G. The role of cytoskeleton networks on lipid-mediated delivery of DNA. Ther. Deliv. 2013; 4:191–202. [PubMed: 23343159]

99. Helenius A, Mellman I, Wall D, Hubbard A. Endosomes. Trends Biochem. Sci. 1983; 8:245–250.

100. Babst M, Odorizzi G. The balance of protein expression and degradation: an ESCRTs point of view. Curr. Opin. Cell Biol. 2013; 25:489–494. [PubMed: 23773569]

101. Luzio JP, Pryor PR, Bright NA. Lysosomes: fusion and function. Nat. Rev. Mol. Cell Biol. 2007; 8:622–632. [PubMed: 17637737]

102. Dominska M, Dykxhoorn DM. Breaking down the barriers: siRNA delivery and endosome escape. J. Cell Sci. 2010; 123:1183–1189. [PubMed: 20356929]

103. Aubry L, Klein G, Martiel JL, Satre M. Kinetics of Endosomal Ph Evolution in Dictyostelium-Discoideum Amebas - Study by Fluorescence Spectroscopy. J. Cell Sci. 1993; 105:861–866. [PubMed: 7691851]

104. Grant BD, Donaldson JG. Pathways and mechanisms of endocytic recycling. Nat. Rev. Mol. Cell Biol. 2009; 10:597–608. [PubMed: 19696797]

105. Sahay G, Querbes W, Alabi C, Eltoukhy A, Sarkar S, Zurenko C, Karagiannis E, Love K, Chen D, Zoncu R, Buganim Y, Schroeder A, Langer R, Anderson DG. Efficiency of siRNA delivery by lipid nanoparticles is limited by endocytic recycling. Nat. Biotechnol. 2013; 31:653–658. [PubMed: 23792629]

106. Pirie CM, Hackel BJ, Rosenblum MG, Wittrup KD. Convergent potency of internalized gelonin immunotoxins across varied cell lines, antigens, and targeting moieties. J. Biol. Chem. 2011; 286:4165–4172. [PubMed: 21138845]

107. Kau TR, Way JC, Silver PA. Nuclear transport and cancer: From mechanism to intervention. Nat. Rev. Cancer. 2004; 4:106–117. [PubMed: 14732865]

108. Wente SR. Gatekeepers of the nucleus. Science. 2000; 288:1374–1377. [PubMed: 10827939]

109. Alvisi G, Poon IK, Jans DA. Tumor-specific nuclear targeting: promises for anti-cancer therapy? Drug Resist. Updat. 2006; 9:40–50. [PubMed: 16621677]

110. Harel A, Forbes DJ. Importin beta: Conducting a much larger cellular symphony. Mol. Cell. 2004; 16:319–330. [PubMed: 15525506]

111. Kurihara D, Akita H, Kudo A, Masuda T, Futaki S, Harashima H. Effect of Polyethyleneglycol Spacer on the Binding Properties of Nuclear Localization Signal-Modified Liposomes to Isolated Nucleus. Biol. Pharm. Bull. 2009; 32:1303–1306. [PubMed: 19571404]

112. Nakamura T, Moriguchi R, Kogure K, Minoura A, Masuda T, Akita H, Kato K, Hamada H, Futaki S, Harashima H. Delivery of condensed DNA by liposomal non-viral gene delivery system into nucleus of dendritic cells. Biol. Pharm. Bull. 2006; 29:1290–1293. [PubMed: 16755037]

113. Grimm D. Small silencing RNAs: state-of-the-art. Adv. Drug Deliv. Rev. 2009; 61:672–703. [PubMed: 19427885]

114. Tang G. siRNA and miRNA: an insight into RISCs. Trends Biochem. Sci. 2005; 30:106–114. [PubMed: 15691656]

115. Khvorova A, Reynolds A, Jayasena SD. Functional siRNAs and miRNAs exhibit strand bias. Cell. 2003; 115:209–216. [PubMed: 14567918]

116. Martinez J, Patkaniowska A, Urlaub H, Luhrmann R, Tuschl T. Single-stranded antisense siRNAs guide target RNA cleavage in RNAi. Cell. 2002; 110:563–574. [PubMed: 12230974]

117. Myers JW, Jones JT, Meyer T, Ferrell JE Jr. Recombinant Dicer efficiently converts large dsRNAs into siRNAs suitable for gene silencing. Nat. Biotechnol. 2003; 21:324–328. [PubMed: 12592410]

118. Schwarz DS, Hutvagner G, Haley B, Zamore PD. Evidence that siRNAs function as guides, not primers, in the Drosophila and human RNAi pathways. Mol. Cell. 2002; 10:537–548. [PubMed: 12408822]

119. Siomi H, Siomi MC. RISC hitches onto endosome trafficking. Nat. Cell Biol. 2009; 11:1049–1051. [PubMed: 19724258]

120. Akhtar S, Benter I. Toxicogenomics of non-viral drug delivery systems for RNAi: Potential impact on siRNA-mediated gene silencing activity and specificity. Adv. Drug Deliv. Rev. 2007; 59:164–182. [PubMed: 17481774]

121. Layzer JM, McCaffrey AP, Tanner AK, Huang Z, Kay MA, Sullenger BA. In vivo activity of nuclease-resistant siRNAs. RNA. 2004; 10:766–771. [PubMed: 15100431]

122. Bumcrot D, Manoharan M, Koteliansky V, Sah DW. RNAi therapeutics: a potential new class of pharmaceutical drugs. Nat. Chem. Biol. 2006; 2:711–719. [PubMed: 17108989]

123. Santel A, Aleku M, Keil O, Endruschat J, Esche V, Fisch G, Dames S, Loffler K, Fechtner M, Arnold W, Giese K, Klippel A, Kaufmann J. A novel siRNA-lipoplex technology for RNA interference in the mouse vascular endothelium. Gene Ther. 2006; 13:1222–1234. [PubMed: 16625243]

124. van de Water FM, Boerman OC, Wouterse AC, Peters JG, Russel FG, Masereeuw R. Intravenously administered short interfering RNA accumulates in the kidney and selectively suppresses gene function in renal proximal tubules. Drug Metab Dispos. 2006; 34:1393–1397. [PubMed: 16714375]

125. Whitehead KA, Langer R, Anderson DG. Knocking down barriers: advances in siRNA delivery. Nat. Rev. Drug Discov. 2009; 8:129–138. [PubMed: 19180106]

126. Goula D, Becker N, Lemkine GF, Normandie P, Rodrigues J, Mantero S, Levi G, Demeneix BA. Rapid crossing of the pulmonary endothelial barrier by polyethylenimine/DNA complexes. Gene Ther. 2000; 7:499–504. [PubMed: 10757023]

127. Gilleron J, Querbes W, Zeigerer A, Borodovsky A, Marsico G, Schubert U, Manygoats K, Seifert S, Andree C, Stoter M, Epstein-Barash H, Zhang L, Koteliansky V, Fitzgerald K, Fava E, Bickle M, Kalaidzidis Y, Akinc A, Maier M, Zerial M. Image-based analysis of lipid nanoparticle-mediated siRNA delivery, intracellular trafficking and endosomal escape. Nat. Biotechnol. 2013; 31:638–646. [PubMed: 23792630]

128. Lee YS, Pressman S, Andress AP, Kim K, White JL, Cassidy JJ, Li X, Lubell K, Lim DH, Cho IS. Silencing by small RNAs is linked to endosomal trafficking. Nat. Cell Biol. 2009; 11:1150–1156. [PubMed: 19684574]

129. Gibbings DJ, Ciaudo C, Erhardt M, Voinnet O. Multivesicular bodies associate with components of miRNA effector complexes and modulate miRNA activity. Nat. Cell Biol. 2009; 11:1143–1149. [PubMed: 19684575]

130. Bartlett DW, Davis ME. Insights into the kinetics of siRNA-mediated gene silencing from live-cell and live-animal bioluminescent imaging. Nucleic Acids Res. 2006; 34:322–333. [PubMed: 16410612]

131. Wittrup A, Ai A, Liu X, Hamar P, Trifonova R, Charisse K, Manoharan M, Kirchhausen T, Lieberman J. Visualizing lipid-formulated siRNA release from endosomes and target gene knockdown. Nat. Biotechnol. 2015; 33:870–876. [PubMed: 26192320]

132. Chang J, Jallouli Y, Kroubi M, Yuan XB, Feng W, Kang CS, Pu PY, Betbeder D. Characterization of endocytosis of transferrin-coated PLGA nanoparticles by the blood-brain barrier. Int. J. Pharm. 2009; 379:285–292. [PubMed: 19416749]

133. Futaki S. Arginine-rich peptides: potential for intracellular delivery of macromolecules and the mystery of the translocation mechanisms. Int. J. Pharm. 2002; 245:1–7. [PubMed: 12270237]

134. Gupta B, Torchilin VP. Transactivating transcriptional activator-mediated drug delivery. Expert. Opin. Drug Deliv. 2006; 3:177–190. [PubMed: 16506946]

135. Yuan JP, Kramer A, Eckerdt F, Kaufmann M, Strebhardt K. Efficient internalization of the polo-box of polo-like kinase 1 fused to an antennapedia peptide results in inhibition of cancer cell proliferation. Cancer Res. 2002; 62:4186–4190. [PubMed: 12154015]

136. Padari K, Saalik P, Hansen M, Koppel K, Raid R, Langel I, Pooga M. Cell transduction pathways of transportans. Bioconjug. Chem. 2005; 16:1399–1410. [PubMed: 16287236]

137. Bechara C, Sagan S. Cell-penetrating peptides: 20 years later, where do we stand? FEBS Lett. 2013; 587:1693–1702. [PubMed: 23669356]

138. Heitz F, Morris MC, Divita G. Twenty years of cell-penetrating peptides: from molecular mechanisms to therapeutics. Br. J. Pharmacol. 2009; 157:195–206. [PubMed: 19309362]

139. Console S, Marty C, Garcia-Echeverria C, Schwendener R, Ballmer-Hofer K. Antennapedia and HIV transactivator of transcription (TAT) "protein transduction domains" promote endocytosis of high molecular weight cargo upon binding to cell surface glycosaminoglycans. Journal of Biological Chemistry. 2003; 278:35109–35114. [PubMed: 12837762]

140. Vives E, Richard JP, Rispal C, Lebleu B. TAT peptide internalization: Seeking the mechanism of entry. Current Protein & Peptide Science. 2003; 4:125–132. [PubMed: 12678851]

141. Wadia JS, Stan RV, Dowdy SF. Transducible TAT-HA fusogenic peptide enhances escape of TAT-fusion proteins after lipid raft macropinocytosis. Nature Medicine. 2004; 10:310–315.

142. Nakase I, Hirose H, Tanaka G, Tadokoro A, Kobayashi S, Takeuchi T, Futaki S. Cell-surface Accumulation of Flock House Virus-derived Peptide Leads to Efficient Internalization via Macropinocytosis. Molecular Therapy. 2009; 17:1868–1876. [PubMed: 19707187]

143. Vendeville A, Rayne F, Bonhoure A, Bettache N, Montcourrier P, Beaumelle B. HIV-1 Tat enters T cells using coated pits before translocating from acidified endosomes and eliciting biological responses. Mol. Biol. Cell. 2004; 15:2347–2360. [PubMed: 15020715]

144. Fittipaldi A, Ferrari A, Zoppe M, Arcangeli C, Pellegrini V, Beltram F, Giacca M. Cell membrane lipid rafts mediate caveolar endocytosis of HIV-1 Tat fusion proteins. Journal of Biological Chemistry. 2003; 278:34141–34149. [PubMed: 12773529]

145. Raagel H, Saalik P, Hansen M, Langel U, Pooga M. CPP-protein constructs induce a population of non-acidic vesicles during trafficking through endo-lysosomal pathway. J. Control. Release. 2009; 139:108–117. [PubMed: 19577599]

146. Wang M, Miller AD, Thanou M. Effect of surface charge and ligand organization on the specific cell-uptake of uPAR-targeted nanoparticles. J. Drug Target. 2013; 21:684–692. [PubMed: 23773028]

147. Sapra P, Allen TM. Internalizing antibodies are necessary for improved therapeutic efficacy of antibody-targeted liposomal drugs. Cancer Res. 2002; 62:7190–7194. [PubMed: 12499256]

148. Davis ME, Chen ZG, Shin DM. Nanoparticle therapeutics: an emerging treatment modality for cancer. Nat. Rev. Drug Discov. 2008; 7:771–782. [PubMed: 18758474]

149. Wang M, Thanou M. Targeting nanoparticles to cancer. Pharmacol. Res. 2010; 62:90–99. [PubMed: 20380880]

150. Mustata RC, Grigorescu A, Petrescu SM. Encapsulated cargo internalized by fusogenic liposomes partially overlaps the endoplasmic reticulum. J. Cell. Molec. Med. 2009; 13:3110–3121. [PubMed: 19438814]

151. Kanasty R, Dorkin JR, Vegas A, Anderson D. Delivery materials for siRNA therapeutics. Nat. Mater. 2013; 12:967–977. [PubMed: 24150415]

152. Varkouhi AK, Scholte M, Storm G, Haisma HJ. Endosomal escape pathways for delivery of biologicals. J. Control Release. 2011; 151:220–228. [PubMed: 21078351]

153. Li WJ, Nicol F, Szoka FC. GALA: a designed synthetic pH-responsive amphipathic peptide with applications in drug and gene delivery. Adv. Drug Deliv. Rev. 2004; 56:967–985. [PubMed: 15066755]

154. Nicol F, Nir S, Szoka FC. Effect of phospholipid composition on an amphipathic peptide-mediated pore formation in bilayer vesicles. Biophys. J. 2000; 78:818–829. [PubMed: 10653794]

155. Nir S, Nieva JL. Interactions of peptides with liposomes: pore formation and fusion. Prog. Lipid Res. 2000; 39:181–206. [PubMed: 10775764]

156. Kakudo T, Chaki S, Futaki S, Nakase I, Akaji K, Kawakami T, Maruyama K, Kamiya H, Harashima H. Transferrin-modified liposomes equipped with a pH-sensitive fusogenic peptide: An artificial viral-like delivery system. Biochemistry. 2004; 43:5618–5628. [PubMed: 15134436]

157. Sasaki K, Kogure K, Chaki S, Nakamura Y, Moriguchi R, Hamada H, Danev R, Nagayama K, Futaki S, Harashima H. An artificial virus-like nano carrier system: enhanced endosomal escape of nanoparticles via synergistic action of pH-sensitive fusogenic peptide derivatives. Anal. Bioanal. Chem. 2008; 391:2717–2727. [PubMed: 18351325]

158. Kaneda Y. Virosomes: evolution of the liposome as a targeted drug delivery system. Adv. Drug Deliv. Rev. 2000; 43:197–205. [PubMed: 10967226]

159. Sarkar DP, Ramani K, Tyagi SK. Targeted gene delivery by virosomes. Methods Mol. Biol. 2002; 199:163–173. [PubMed: 12094567]

160. Moser C, Metcalfe IC, Viret JF. Virosomal adjuvanted antigen delivery systems. Expert. Rev. Vaccines. 2003; 2:189–196. [PubMed: 12899570]

161. Mastrobattista E, Koning GA, van Bloois L, Filipe ACS, Jiskoot W, Storm G. Functional characterization of an endosome-disruptive peptide and its application in cytosolic delivery of immunoliposome-entrapped proteins. J. Biol. Chem. 2002; 277:27135–27143. [PubMed: 12021269]

162. Plank C, Oberhauser B, Mechtler K, Koch C, Wagner E. The influence of endosome-disruptive peptides on gene transfer using synthetic virus-like gene transfer systems. J. Biol. Chem. 1994; 269:12918–12924. [PubMed: 8175709]

163. Kakimoto S, Hamada T, Komatsu Y, Takagi M, Tanabe T, Azuma H, Shinkai S, Nagasaki T. The conjugation of diphtheria toxin T domain to poly(ethylenimine) based vectors for enhanced endosomal escape during gene transfection. Biomaterials. 2009; 30:402–408. [PubMed: 18930314]

164. Kwon EJ, Bergen JM, Pun SH. Application of an HIV gp41-derived peptide for enhanced intracellular trafficking of synthetic gene and siRNA delivery vehicles. Bioconjug. Chem. 2008; 19:920–927. [PubMed: 18376855]

165. Simoes S, Moreira JN, Fonseca C, Duzgunes N, de Lima MCP. On the formulation of pH-sensitive long circulation times. Adv. Drug Deliv. Rev. 2004; 56:947–965. [PubMed: 15066754]

166. Foerg C, Ziegler U, Fernandez-Carneado J, Giralt E, Rennert R, Beck-Sickinger AG, Merkle HP. Decoding the entry of two novel cell-penetrating peptides in HeLa cells: Lipid raft-mediated endocytosis and endosomal escape. Biochemistry. 2005; 44:72–81. [PubMed: 15628847]

167. Song LY, Ahkong QF, Rong Q, Wang Z, Ansell S, Hope MJ, Mui B. Characterization of the inhibitory effect of PEG-lipid conjugates on the intracellular delivery of plasmid and antisense DNA mediated by cationic lipid liposomes. Biochim. Biophys. Acta-Biomembr. 2002; 1558:1–13.

168. Boomer JA, Qualls MM, Inerowicz HD, Haynes RH, Patri VS, Kim JM, Thompson DH. Cytoplasmic Delivery of Liposomal Contents Mediated by an Acid-Labile Cholesterol-Vinyl Ether-PEG Conjugate. Bioconjug. Chem. 2009; 20:47–59. [PubMed: 19072698]

169. Xu H, Deng YH, Chen DW, Hong WW, Lu Y, Dong XH. Esterase-catalyzed dePEGylation of pH-sensitive vesicles modified with cleavable PEG-lipid derivatives. J. Control. Release. 2008; 130:238–245. [PubMed: 18657874]

170. Maeda T, Fujimoto K. A reduction-triggered delivery by a liposomal carrier possessing membrane-permeable ligands and a detachable coating. Colloids Surf. B Biointerfaces. 2006; 49:15–21. [PubMed: 16574385]

171. Capriotti AL, Caracciolo G, Caruso G, Cavaliere C, Pozzi D, Samperi R, Lagan+á A. Analysis of plasma protein adsorption onto DC-Chol-DOPE cationic liposomes by HPLC-CHIP coupled to a Q-TOF mass spectrometer. Anal. Bioanal. Chem. 2010; 398:2895–2903. [PubMed: 20859620]

172. Westmeier D, Chen C, Stauber RH, Docter D. The bio-corona and its impact on nanomaterial toxicity. Eur. J. Nanomed. 2015; 7:153–168.

173. Lynch I, Ahluwalia A, Boraschi D, Byrne HJ, Fadeel B, Gehr P, Gutleb AC, Kendall M, Papadopoulos MG. The bio-nano-interface in predicting nanoparticle fate and behaviour in living organisms: towards grouping and categorising nanomaterials and ensuring nanosafety by design. BioNanoMaterials. 2013; 14:195–216.

174. Capriotti AL, Caracciolo G, Caruso G, Foglia P, Pozzi D, Samperi R, Lagan+á A. DNA affects the composition of lipoplex protein corona: a proteomics approach. Proteomics. 2011; 11:3349–3358. [PubMed: 21751361]

175. Sasidharan A, Riviere JE, Monteiro-Riviere NA. Gold and silver nanoparticle interactions with human proteins: impact and implications in biocorona formation. J. Mater. Chem. B. 2015; 3:2075–2082.

176. Sempf K, Arrey T, Gelperina S, Schorge T, Meyer B, Karas M, Kreuter J. Adsorption of plasma proteins on uncoated PLGA nanoparticles. Eur. J. Pharm. Biopharm. 2013; 85:53–60. [PubMed: 23395970]

177. Tenzer S, Docter D, Kuharev J, Musyanovych A, Fetz V, Hecht R, Schlenk F, Fischer D, Kiouptsi K, Reinhardt C, Landfester K, Schild H, Maskos M, Knauer SK, Stauber RH. Rapid formation of plasma protein corona critically affects nanoparticle pathophysiology. Nat. Nanotechnol. 2013; 8:772–781. [PubMed: 24056901]

178. Monopoli MP, Walczyk D, Campbell A, Elia G, Lynch I, Baldelli Bombelli F, Dawson KA. Physical and chemical aspects of protein corona: relevance to in vitro and in vivo biological impacts of nanoparticles. J. Am. Chem. Soc. 2011; 133:2525–2534. [PubMed: 21288025]

179. Shannahan, JH. Nanoparticle biocorona. In: Bhushan, B., editor. Encyclopedia of Nanotechnology. Netherlands: Springer; 2015. p. 1-4.

180. Monopoli MP, Aberg C, Salvati A, Dawson KA. Biomolecular coronas provide the biological identity of nanosized materials. Nat Nanotechnol. 2012; 7:779–786. [PubMed: 23212421]

181. Gessner A, Olbrich C, Schroder W, Kayser O, Muller RH. The role of plasma proteins in brain targeting: species dependent protein adsorption patterns on brain-specific lipid drug conjugate (LDC) nanoparticles. Int. J. Pharm. 2001; 214:87–91. [PubMed: 11282243]

182. Goppert TM, Muller RH. Polysorbate-stabilized solid lipid nanoparticles as colloidal carriers for intravenous targeting of drugs to the brain: comparison of plasma protein adsorption patterns. J. Drug Target. 2005; 13:179–187. [PubMed: 16036306]

183. Kasongo KW, Jansch M, Muller RH, Walker RB. Evaluation of the in vitro differential protein adsorption patterns of didanosine-loaded nanostructured lipid carriers (NLCs) for potential targeting to the brain. J. Liposome Res. 2011; 21:245–254. [PubMed: 21174528]

184. Kim HR, Andrieux K, Delomenie C, Chacun H, Appel M, Desmaele D, Taran F, Georgin D, Couvreur P, Taverna M. Analysis of plasma protein adsorption onto PEGylated nanoparticles by complementary methods: 2-DE, CE and Protein Lab-on-chip system. Electrophoresis. 2007; 28:2252–2261. [PubMed: 17557357]

185. Kratzer I, Wernig K, Panzenboeck U, Bernhart E, Reicher H, Wronski R, Windisch M, Hammer A, Malle E, Zimmer A, Sattler W. Apolipoprotein A-I coating of protamine-oligonucleotide nanoparticles increases particle uptake and transcytosis in an in vitro model of the blood-brain barrier. J. Control Release. 2007; 117:301–311. [PubMed: 17239472]

186. Kreuter J, Shamenkov D, Petrov V, Ramge P, Cychutek K, Koch-Brandt C, Alyautdin R. Apolipoprotein-mediated transport of nanoparticle-bound drugs across the blood-brain barrier. J. Drug Target. 2002; 10:317–325. [PubMed: 12164380]

187. Kreuter J. Influence of the surface properties on nanoparticle-mediated transport of drugs to the brain. J. Nanosci. Nanotechnol. 2004; 4:484–488. [PubMed: 15503433]

188. Kreuter J. Mechanism of polymeric nanoparticle-based drug transport across the blood-brain barrier (BBB). J. Microencapsul. 2013; 30:49–54. [PubMed: 22676632]

189. Mariam J, Sivakami S, Dongre PM. Albumin corona on nanoparticles - a strategic approach in drug delivery. Drug Deliv. 2015:1–9. [PubMed: 26056719]

190. Ogawara K, Furumoto K, Nagayama S, Minato K, Higaki K, Kai T, Kimura T. Pre-coating with serum albumin reduces receptor-mediated hepatic disposition of polystyrene nanosphere: implications for rational design of nanoparticles. J. Control Release. 2004; 100:451–455. [PubMed: 15567509]

191. Bargheer D, Nielsen J, Gebel G, Heine M, Salmen SC, Stauber R, Weller H, Heeren J, Nielsen P. The fate of a designed protein corona on nanoparticles in vitro and in vivo. Beilstein. J. Nanotechnol. 2015; 6:36–46. [PubMed: 25671150]

192. Dobrovolskaia MA, Neun BW, Man S, Ye X, Hansen M, Patri AK, Crist RM, McNeil SE. Protein corona composition does not accurately predict hematocompatibility of colloidal gold nanoparticles. Nanomedicine. 2014; 10:1453–1463. [PubMed: 24512761]

193. Nuytten N, Hakimhashemi M, Ysenbaert T, Defour L, Trekker J, Soenen SJ, Van der Meeren P, De CM. PEGylated lipids impede the lateral diffusion of adsorbed proteins at the surface of (magneto)liposomes. Colloids Surf. B Biointerfaces. 2010; 80:227–231. [PubMed: 20630718]

194. Pelaz B, Del PP, Maffre P, Hartmann R, Gallego M, Rivera-Fernandez S, de la Fuente JM, Nienhaus GU, Parak WJ. Surface Functionalization of Nanoparticles with Polyethylene Glycol: Effects on Protein Adsorption and Cellular Uptake. ACS Nano. 2015; 9:6996–7008. [PubMed: 26079146]

195. Walkey CD, Olsen JB, Guo H, Emili A, Chan WC. Nanoparticle size and surface chemistry determine serum protein adsorption and macrophage uptake. J. Am. Chem. Soc. 2012; 134:2139–2147. [PubMed: 22191645]

196. Mastorakos P, Zhang C, Berry S, Oh Y, Lee S, Eberhart CG, Woodworth GF, Suk JS, Hanes J. Highly PEGylated DNA nanoparticles provide uniform and widespread gene transfer in the brain. Adv. Healthc. Mater. 2015; 4:1023–1033. [PubMed: 25761435]

197. Buyens K, Lucas B, Raemdonck K, Braeckmans K, Vercammen J, Hendrix J, Engelborghs Y, De Smedt SC, Sanders NN. A fast and sensitive method for measuring the integrity of siRNA-carrier complexes in full human serum. J. Control. Release. 2008; 126:67–76. [PubMed: 18068258]

198. Caracciolo G, Callipo L, De Sanctis SC, Cavaliere C, Pozzi D, Lagan A. Surface adsorption of protein corona controls the cell internalization mechanism of DC-Chol DOPE/DNA lipoplexes in serum. Biochim. Biophys. Acta-Biomembr. 2010; 1798:536–543.

199. Ziello JE, Huang Y, Jovin IS. Cellular endocytosis and gene delivery. Mol. Med. 2010; 16:222–229. [PubMed: 20454523]

200. Caracciolo G, Pozzi D, Capriotti AL, Cavaliere C, Foglia P, Amenitsch H, Lagan+á A. Evolution of the protein corona of lipid gene vectors as a function of plasma concentration. Langmuir. 2011; 27:15048–15053. [PubMed: 22043822]

201. Hanash S. Disease proteomics. Nature. 2003; 422:226–232. [PubMed: 12634796]

202. Conrads TP, Fusaro VA, Ross S, Johann D, Rajapakse V, Hitt BA, Steinberg SM, Kohn EC, Fishman DA, Whitely G, Barrett JC, Liotta LA, Petricoin EF III, Veenstra TD. High-resolution serum proteomic features for ovarian cancer detection. Endocr. Relat Cancer. 2004; 11:163–178. [PubMed: 15163296]

203. Clift MJ, Rothen-Rutishauser B, Brown DM, Duffin R, Donaldson K, Proudfoot L, Guy K, Stone V. The impact of different nanoparticle surface chemistry and size on uptake and toxicity in a murine macrophage cell line. Toxicol. Appl. Pharmacol. 2008; 232:418–427. [PubMed: 18708083]

204. Ruge CA, Schaefer UF, Herrmann J, Kirch J, Canadas O, Echaide M, Perez-Gil J, Casals C, Muller R, Lehr CM. The interplay of lung surfactant proteins and lipids assimilates the macrophage clearance of nanoparticles. PLoS. One. 2012; 7:e40775. [PubMed: 22802970]

205. Monteiro-Riviere NA, Samberg ME, Oldenburg SJ, Riviere JE. Protein binding modulates the cellular uptake of silver nanoparticles into human cells: implications for in vitro to in vivo extrapolations? Toxicol. Lett. 2013; 220:286–293. [PubMed: 23660336]

206. Riviere JE. Of mice, men and nanoparticle biocoronas: are in vitro to in vivo correlations and interspecies extrapolations realistic? Nanomedicine. 2013; 8:1357–1359. [PubMed: 23987106]

207. Walczyk D, Bombelli FB, Monopoli MP, Lynch I, Dawson KA. What the cell sees in bionanoscience. J. Am. Chem. Soc. 2010; 132:5761–5768. [PubMed: 20356039]

208. O'Brien ME, Wigler N, Inbar M, Rosso R, Grischke E, Santoro A, Catane R, Kieback DG, Tomczak P, Ackland SP, Orlandi F, Mellars L, Alland L, Tendler C. Reduced cardiotoxicity and comparable efficacy in a phase III trial of pegylated liposomal doxorubicin HCl (CAELYX/Doxil) versus conventional doxorubicin for first-line treatment of metastatic breast cancer. Ann. Oncol. 2004; 15:440–449. [PubMed: 14998846]

209. Northfelt DW, Dezube BJ, Thommes JA, Miller BJ, Fischl MA, Friedman-Kien A, Kaplan LD, Du MC, Mamelok RD, Henry DH. Pegylated-liposomal doxorubicin versus doxorubicin, bleomycin, and vincristine in the treatment of AIDS-related Kaposi's sarcoma: results of a randomized phase III clinical trial. J. Clin. Oncol. 1998; 16:2445–2451. [PubMed: 9667262]

210. Gill PS, Wernz J, Scadden DT, Cohen P, Mukwaya GM, von Roenn JH, Jacobs M, Kempin S, Silverberg I, Gonzales G, Rarick MU, Myers AM, Shepherd F, Sawka C, Pike MC, Ross ME. Randomized phase III trial of liposomal daunorubicin versus doxorubicin, bleomycin, and vincristine in AIDS-related Kaposi's sarcoma. J. Clin. Oncol. 1996; 14:2353–2364. [PubMed: 8708728]

211. Prabhakar U, Maeda H, Jain RK, Sevick-Muraca EM, Zamboni W, Farokhzad OC, Barry ST, Gabizon A, Grodzinski P, Blakey DC. Challenges and key considerations of the enhanced permeability and retention effect for nanomedicine drug delivery in oncology. Cancer Res. 2013; 73:2412–2417. [PubMed: 23423979]

212. Hendriks BS, Reynolds JG, Klinz SG, Geretti E, Lee H, Leonard SC, Gaddy DF, Espelin CW, Nielsen UB, Wickham TJ. Multiscale kinetic modeling of liposomal Doxorubicin delivery quantifies the role of tumor and drug-specific parameters in local delivery to tumors. CPT. Pharmacometrics. Syst. Pharmacol. 2012; 1:e15. [PubMed: 23835797]

213. Fridman WH, Pages F, Sautes-Fridman C, Galon J. The immune contexture in human tumours: impact on clinical outcome. Nat. Rev. Cancer. 2012; 12:298–306. [PubMed: 22419253]

214. Mlecnik B, Tosolini M, Kirilovsky A, Berger A, Bindea G, Meatchi T, Bruneval P, Trajanoski Z, Fridman WH, Pages F, Galon J. Histopathologic-based prognostic factors of colorectal cancers are associated with the state of the local immune reaction. J Clin. Oncol. 2011; 29:610–618. [PubMed: 21245428]

215. Chen DS, Mellman I. Oncology meets immunology: the cancer-immunity cycle. Immunity. 2013; 39:1–10. [PubMed: 23890059]

216. Joyce JA, Fearon DT. T cell exclusion, immune privilege, and the tumor microenvironment. Science. 2015; 348:74–80. [PubMed: 25838376]

217. Ley K, Laudanna C, Cybulsky MI, Nourshargh S. Getting to the site of inflammation: the leukocyte adhesion cascade updated. Nat. Rev. Immunol. 2007; 7:678–689. [PubMed: 17717539]

218. Peranzoni E, Rivas-Caicedo A, Bougherara H, Salmon H, Donnadieu E. Positive and negative influence of the matrix architecture on antitumor immune surveillance. Cell Mol. Life Sci. 2013; 70:4431–4448. [PubMed: 23649148]

219. Ribas A. Tumor immunotherapy directed at PD-1. N. Engl. J. Med. 2012; 366:2517–2519. [PubMed: 22658126]

220. OncLive staff. The role of Anti-PD-L1 immunotherapy in cancer. Http://Www.Onclive.Com/Web-Exclusives/the-Role-of-Anti-Pd-L1-Immunotherapy-in-Cancer.

221. Sharma P, Allison JP. The future of immune checkpoint therapy. Science. 2015; 348:56–61. [PubMed: 25838373]

222. Yaqub F. Nivolumab for squamous-cell non-small-cell lung cancer. Lancet Oncol. 2015; 16:e319. [PubMed: 26062776]

223. BMS. Package insert Opdivo (nivolumab). 2014 hHttp://Packageinserts.Bms.Com/Pi/Pi_Opdivo.Pdf.

224. Merck. Package insert Keytruda (pembrolizumab). 2014. Http://Www.Accessdata.Fda.Gov/Drugsatfda_Docs/Label/2014/125514lbl.Pdf

225. Hodi FS, O'Day SJ, McDermott DF, Weber RW, Sosman JA, Haanen JB, Gonzalez R, Robert C, Schadendorf D, Hassel JC, Akerley W, van den Eertwegh AJ, Lutzky J, Lorigan P, Vaubel JM, Linette GP, Hogg D, Ottensmeier CH, Lebbe C, Peschel C, Quirt I, Clark JI, Wolchok JD, Weber JS, Tian J, Yellin MJ, Nichol GM, Hoos A, Urba WJ. Improved survival with ipilimumab in patients with metastatic melanoma. N. Engl. J. Med. 2010; 363:711–723. [PubMed: 20525992]

226. Peske JD, Woods AB, Engelhard VH. Control of CD8 T-Cell Infiltration into Tumors by Vasculature and Microenvironment. Adv. Cancer Res. 2015; 128:263–307. [PubMed: 26216636]

227. Friedl P, Weigelin B. Interstitial leukocyte migration and immune function. Nat. Immunol. 2008; 9:960–969. [PubMed: 18711433]

228. Mrass P, Takano H, Ng LG, Daxini S, Lasaro MO, Iparraguirre A, Cavanagh LL, von Andrian UH, Ertl HC, Haydon PG, Weninger W. Random migration precedes stable target cell interactions of tumor-infiltrating T cells. J Exp. Med. 2006; 203:2749–2761. [PubMed: 17116735]

229. Boissonnas A, Fetler L, Zeelenberg IS, Hugues S, Amigorena S. In vivo imaging of cytotoxic T cell infiltration and elimination of a solid tumor. J Exp. Med. 2007; 204:345–356. [PubMed: 17261634]

230. Salmon H, Franciszkiewicz K, Damotte D, Dieu-Nosjean MC, Validire P, Trautmann A, Mami-Chouaib F, Donnadieu E. Matrix architecture defines the preferential localization and migration of T cells into the stroma of human lung tumors. J Clin. Invest. 2012; 122:899–910. [PubMed: 22293174]

231. Hartmann N, Giese NA, Giese T, Poschke I, Offringa R, Werner J, Ryschich E. Prevailing role of contact guidance in intrastromal T-cell trapping in human pancreatic cancer. Clin. Cancer Res. 2014; 20:3422–3433. [PubMed: 24763614]

232. Bronkhorst IH, Vu TH, Jordanova ES, Luyten GP, Burg SH, Jager MJ. Different subsets of tumor-infiltrating lymphocytes correlate with macrophage influx and monosomy 3 in uveal melanoma. Invest Ophthalmol. Vis. Sci. 2012; 53:5370–5378. [PubMed: 22743317]

233. Norazmi MN, Hohmann AW, Skinner JM, Jarvis LR, Bradley J. Density and phenotype of tumour-associated mononuclear cells in colonic carcinomas determined by computer-assisted video image analysis. Immunology. 1990; 69:282–286. [PubMed: 1968427]

234. Lieubeau B, Heymann MF, Henry F, Barbieux I, Meflah K, Gregoire M. Immunomodulatory effects of tumor-associated fibroblasts in colorectal-tumor development. Int. J Cancer. 1999; 81:629–636. [PubMed: 10225455]

235. Galon J, Pages F, Marincola FM, Angell HK, Thurin M, Lugli A, Zlobec I, Berger A, Bifulco C, Botti G, Tatangelo F, Britten CM, Kreiter S, Chouchane L, Delrio P, Arndt H, Asslaber M, Maio M, Masucci GV, Mihm M, Vidal-Vanaclocha F, Allison JP, Gnjatic S, Hakansson L, Huber C, Singh-Jasuja H, Ottensmeier C, Zwierzina H, Laghi L, Grizzi F, Ohashi PS, Shaw PA, Clarke BA, Wouters BG, Kawakami Y, Hazama S, Okuno K, Wang E, O'Donnell-Tormey J, Lagorce C, Pawelec G, Nishimura MI, Hawkins R, Lapointe R, Lundqvist A, Khleif SN, Ogino S, Gibbs P, Waring P, Sato N, Torigoe T, Itoh K, Patel PS, Shukla SN, Palmqvist R, Nagtegaal ID, Wang Y, D'Arrigo C, Kopetz S, Sinicrope FA, Trinchieri G, Gajewski TF, Ascierto PA, Fox BA. Cancer classification using the Immunoscore: a worldwide task force. J. Transl. Med. 2012; 10:205. [PubMed: 23034130]

236. Miyahira AK, Kissick HT, Bishop JL, Takeda DY, Barbieri CE, Simons JW, Pienta KJ, Soule HR. Beyond immune checkpoint blockade: new approaches to targeting host-tumor interactions in prostate cancer: report from the 2014 Coffey-Holden prostate cancer academy meeting. Prostate. 2015; 75:337–347. [PubMed: 25358693]

237. Smith E, Breznik J, Lichty BD. Strategies to enhance viral penetration of solid tumors. Hum. Gene Ther. 2011; 22:1053–1060. [PubMed: 21443415]

238. Johansson A, Hamzah J, Ganss R. More than a scaffold: Stromal modulation of tumor immunity. Biochim. Biophys. Acta. 2015 Epub ahead of print.

239. Ozcelikkale A, Ghosh S, Han B. Multifaceted transport characteristics of nanomedicine: needs for characterization in dynamic environment. Mol. Pharm. 2013; 10:2111–2126. [PubMed: 23517188]

240. Kim M, Gillies RJ, Rejniak KA. Current advances in mathematical modeling of anti-cancer drug penetration into tumor tissues. Front Oncol. 2013; 3:278. [PubMed: 24303366]

241. Ait-Oudhia S, Straubinger RM, Mager DE. Systems pharmacological analysis of paclitaxel-mediated tumor priming that enhances nanocarrier deposition and efficacy. J. Pharmacol. Exp. Ther. 2013; 344:103–112. [PubMed: 23115220]

242. Ford Versypt AN, Pack DW, Braatz RD. Mathematical modeling of drug delivery from autocatalytically degradable PLGA microspheres--a review. J. Control Release. 2013; 165:29–37. [PubMed: 23103455]

243. Siepmann J, Siepmann F. Modeling of diffusion controlled drug delivery. J. Control Release. 2012; 161:351–362. [PubMed: 22019555]

244. Kalyanasundaram S, Calhoun VD, Leong KW. A finite element model for predicting the distribution of drugs delivered intracranially to the brain. Am. J. Physiol. 1997; 273:R1810–R1821. [PubMed: 9374827]

245. Au JL, Lu Z, Wientjes MG. Versatility of particulate carriers: development of pharmacodynamically optimized drug-loaded microparticles for treatment of peritoneal cancer. AAPS J. 2015; 17:1065–1079. [PubMed: 26089090]

246. Lu Z, Tsai M, Lu D, Wang J, Wientjes MG, Au JL. Tumor penetrating microparticles for intraperitoneal therapy of ovarian cancer. J. Pharmacol. Exp. Ther. 2008; 327:673–682. [PubMed: 18780831]

247. Wang J, Lu Z, Wang J, Cui M, Yeung BZ, Cole DJ, Wientjes MG, Au JL. Paclitaxel tumor priming promotes delivery and transfection of intravenous lipid-siRNA in pancreatic tumors. J. Control Release. 2015; 216:103–110. [PubMed: 26272765]

248. Wong HL, Shen Z, Lu Z, Wientjes MG, Au JL. Paclitaxel tumor-priming enhances siRNA delivery and transfection in 3-dimensional tumor cultures. Mol. Pharm. 2011; 8:833–840. [PubMed: 21417439]

249. Weinberg BD, Patel RB, Exner AA, Saidel GM, Gao J. Modeling doxorubicin transport to improve intratumoral drug delivery to RF ablated tumors. J. Control Release. 2007; 124:11–19. [PubMed: 17900740]

250. Groh CM, Hubbard ME, Jones PF, Loadman PM, Periasamy N, Sleeman BD, Smye SW, Twelves CJ, Phillips RM. Mathematical and computational models of drug transport in tumours. J. R. Soc. Interface. 2014; 11:20131173. [PubMed: 24621814]

251. Kojic, M.; Milosevic, M.; Kojic, N.; Isailovic, V.; Petrovic, D.; Filipovic, N.; Ferrari, M.; Ziemys, A. Transport phenomena: computational models for convective and diffusive transport in capillaries and tissue. In: De, S.; Hwang, W.; Kuhl, E., editors. Multiscale modeling in biomechanics and mechanobiology. ChSpringer; 2015. p. 131-156.

252. Li Y, Stroberg W, Lee TR, Kim HS, Man H, Ho D, Decuzzi P, Liu WK. Multiscale modeling and uncertainty quantification in nanoparticle-mediated drug/gene delivery. Comput. Mech. 2014; 53:511–537.

253. Liu Y, Shah S, Tan J. Computational modeling of nanoparticle targeted drug delivery. Rev. Nanosci. Nanotech. 2015; 1:66–83.

254. Shipley RJ, Chapman SJ. Multiscale modelling of fluid and drug transport in vascular tumours. Bull. Math. Biol. 2010; 72:1464–1491. [PubMed: 20099043]

255. Kim B, Han G, Toley BJ, Kim CK, Rotello VM, Forbes NS. Tuning payload delivery in tumour cylindroids using gold nanoparticles. Nat. Nanotechnol. 2010; 5:465–472. [PubMed: 20383126]

256. Gasselhuber A, Dreher MR, Partanen A, Yarmolenko PS, Woods D, Wood BJ, Haemmerich D. Targeted drug delivery by high intensity focused ultrasound mediated hyperthermia combined with temperature-sensitive liposomes: computational modelling and preliminary in vivovalidation. Int. J. Hyperthermia. 2012; 28:337–348. [PubMed: 22621735]

257. Gao Y, Li M, Chen B, Shen Z, Guo P, Wientjes MG, Au JL. Predictive models of diffusive nanoparticle transport in 3-dimensional tumor cell spheroids. AAPS. J. 2013; 15:816–831. [PubMed: 23605950]

258. Wientjes MG, Yeung BZ, Lu Z, Wientjes MG, Au JL. Predicting diffusive transport of cationic liposomes in 3-dimensional tumor spheroids. J. Control Release. 2014; 192:10–18. [PubMed: 24995948]

259. Au JL, Guo P, Gao Y, Lu Z, Wientjes MG, Tsai M, Wientjes MG. Multiscale tumor spatiokinetic model for intraperitoneal therapy. AAPS J. 2014; 16:424–439. [PubMed: 24570339]

260. Gao Y, Guo P, Lu Z, Tsai M, Wientjes MG, Au JL. Drug transport in peritoneal tumors during intraperitoneal therapy - evaluation by computational model. Proc. Am. Assoc. Cancer Res. 2011

261. Durand RE. Chemosensitivity testing in V79 spheroids: drug delivery and cellular microenvironment. J. Natl. Cancer Inst. 1986; 77:247–252. [PubMed: 2425117]

262. Nederman T, Norling B, Glimelius B, Carlsson J, Brunk U. Demonstration of an extracellular matrix in multicellular tumor spheroids. Cancer Res. 1984; 44:3090–3097. [PubMed: 6373002]

263. Minchinton AI, Tannock IF. Drug penetration in solid tumours. Nat. Rev. Cancer. 2006; 6:583–592. [PubMed: 16862189]

264. Axelsson I. Characterization of proteins and other macromolecules by agarose gel chromatography. J. Chromatogr. 1978; 152:21–32.

265. Barakat RR, Sabbatini P, Bhaskaran D, Revzin M, Smith A, Venkatraman E, Aghajanian C, Hensley M, Soignet S, Brown C, Soslow R, Markman M, Hoskins WJ, Spriggs D. Intraperitoneal chemotherapy for ovarian carcinoma: results of long-term follow-up. J. Clin. Oncol. 2002; 20:694–698. [PubMed: 11821450]

266. Lin MI, Sessa WC. Antiangiogenic therapy: creating a unique "window" of opportunity. Cancer Cell. 2004; 6:529–531. [PubMed: 15607955]

267. Winkler F, Kozin SV, Tong RT, Chae SS, Booth MF, Garkavtsev I, Xu L, Hicklin DJ, Fukumura D, di Tomaso E, Munn LL, Jain RK. Kinetics of vascular normalization by VEGFR2 blockade governs brain tumor response to radiation: role of oxygenation, angiopoietin-1, and matrix metalloproteinases. Cancer Cell. 2004; 6:553–563. [PubMed: 15607960]

268. Jain RK, Tong RT, Munn LL. Effect of vascular normalization, by antiangiogenic therapy on interstitial hypertension, peritumor edema, and lymphatic metastasis: Insights from a mathematical model. Cancer Res. 2007; 67:2729–2735. [PubMed: 17363594]

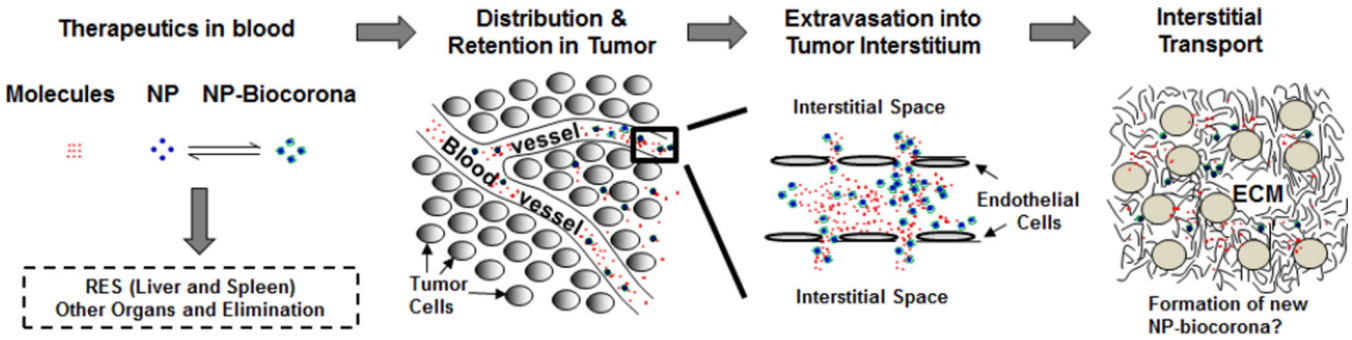

Figure 1. Transport of a therapeutic from injection site to tumors

Following an intravenous injection, therapeutics (small or large molecules, or their NP carriers) are distributed in blood and undergo the following steps: (a) removal from the systemic circulation by cells of reticuloendothelial system (RES) or elimination by metabolism and excretion, (b) transported to organs including tumors *via* the systemic circulation, (c) extravsation (transvascular transport by diffusion or convection) into tissue interstitium, and (d) interstitial transport by diffusion and convection to reach individual tumor cells. Note the formation of NP-biocorona complex in blood due to NP interactions with serum proteins, and the exchange of serum proteins on NP-biocorona with proteins in tumor microenvironment may result in the formation of new NP-biocorona complex. Figure and legend are adapted from Figure 1 of [5] and reprinted with permission.

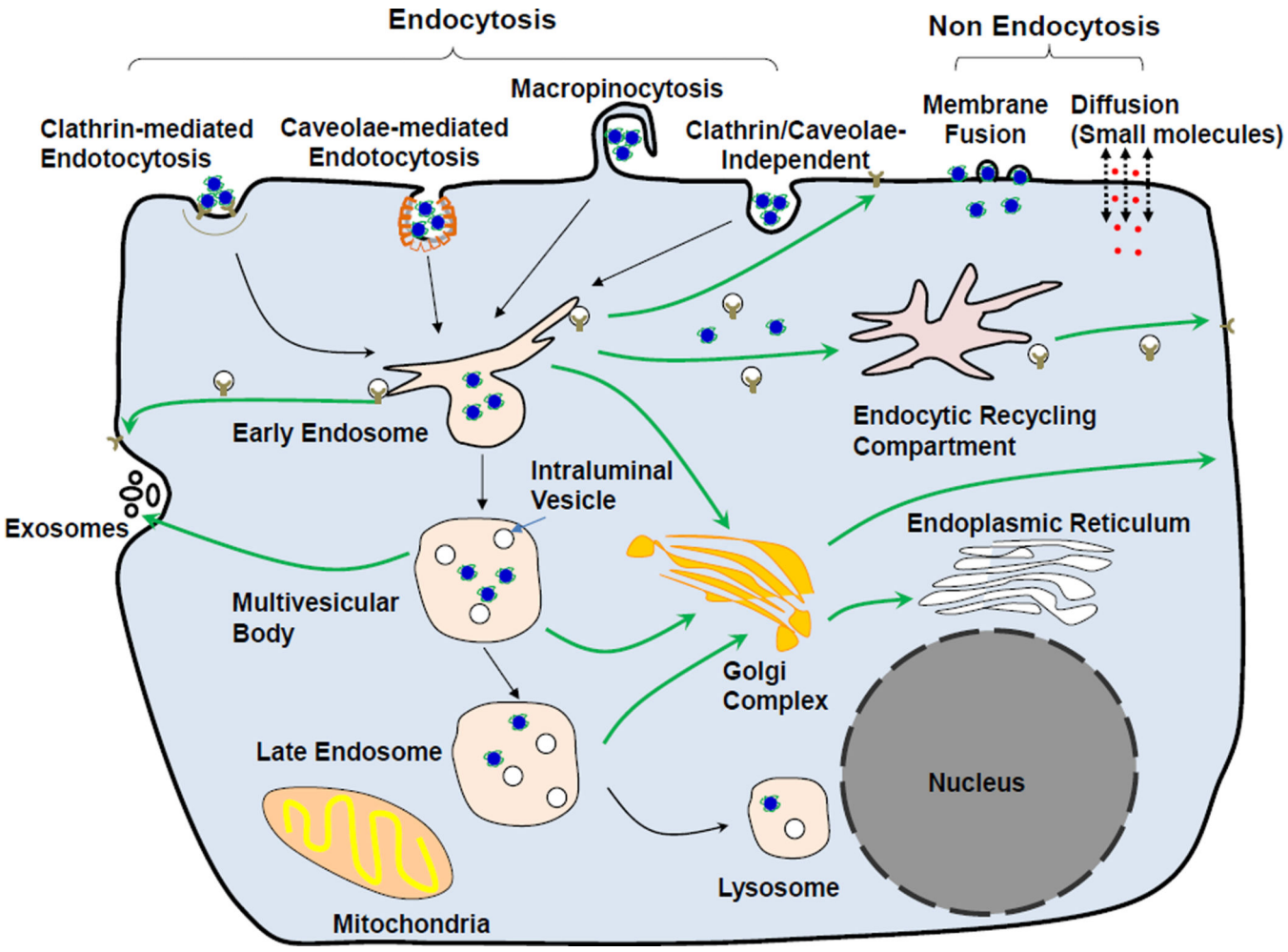

Figure 2. Internalization and intracellular trafficking of therapeutics and nanoparticles

Mechanisms of internalization include (a) non-endocytic pathways: diffusion/active transport of small molecule therapeutics across the cell membranes and fusion of nanoparticles with the cell membrane, and (b) endocytic pathways: clathrin-mediated endocytosis, caveolae-mediated endocytosis, clathrin- and caveolae-independent endocytosis and macropinocytosis. In an endocytic pathway, the cargo is presented to the early endosomes and get sorted into recycling endosomes that are either directly recycled back to the cell membrane or indirectly through the endosome recycling center, or late endosomes that fuse with lysosomes. One aspect of the sorting results in budding of early endosomes to form intraluminal vesicles, a component of multivesicular bodies that either mature into late endosomes or are fused with the cell membrane followed by releasing the intraluminal vesicles and their contents as exosomes. Drawing of subcellular organelles is not to scale. See text for references.

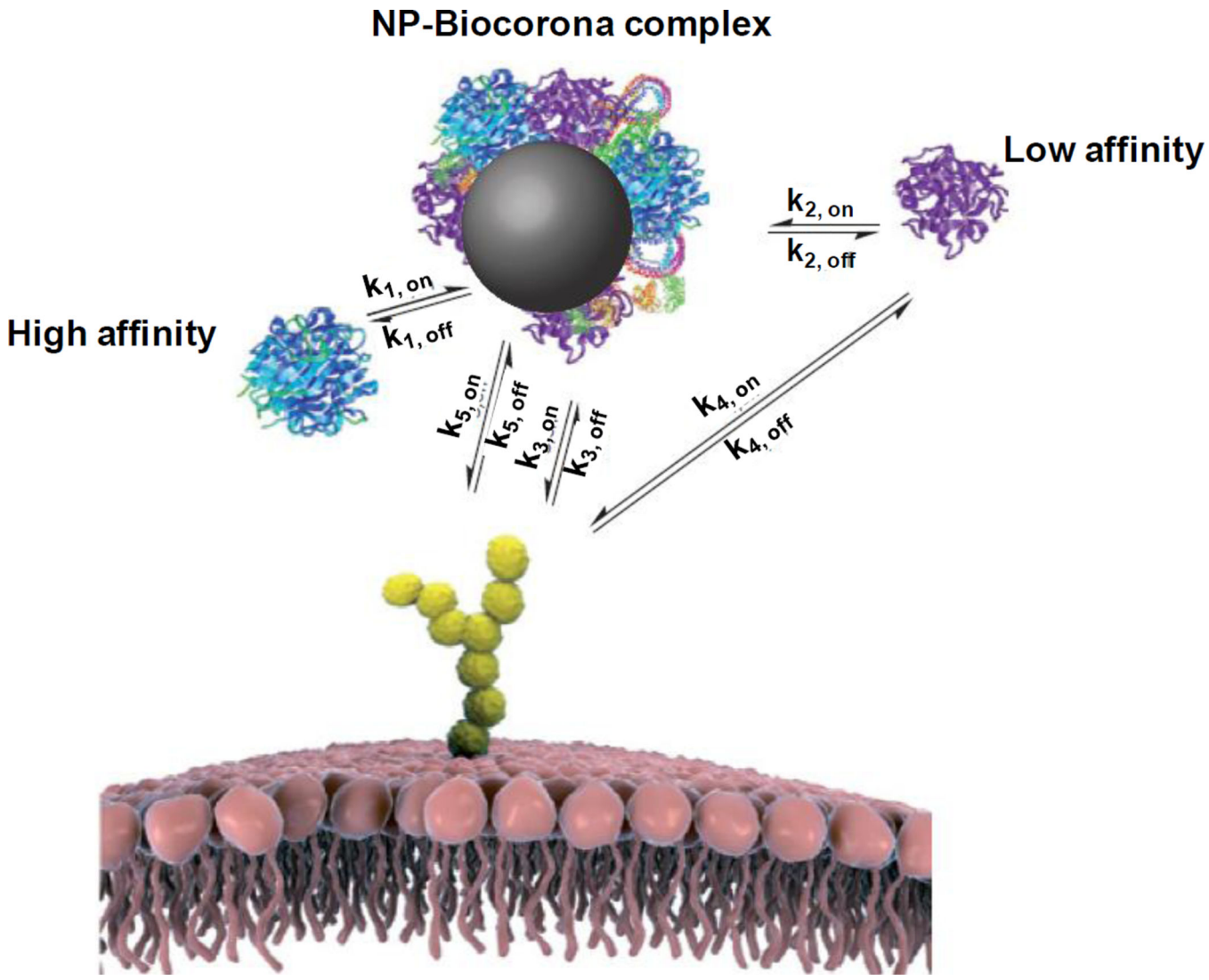

Figure 3. Nanoparticle biocorona

Biomolecules in the biological milieu adsorb strongly to the NP surface (*k*1), forming a tightly bound layer of biocorona in immediate contact with NP (hard corona). Other biomolecules with affinity to the NP-hard biocorona complex (primarily to the hard corona itself) interacts with NP-biocorona at a much lower rate and form a soft biocorona; molecules in the soft biocorona are in rapid exchange with the environment (*k*2). If sufficiently long-lived in the biocorona, a biomolecule may lead to recognition of the NP-biocorona complex as a whole by a cell membrane receptor (*k*3). The same biomolecule alone can also be recognized by the receptor (*k*4). If present, the bare surface of NP may also interact with cell surface receptors (*k*5) or other constituents of the cell membrane. Figure and legend are adapted and reprinted with permission from [180]. Not shown in Figure: Internalization of NP-biocorona complex by the endocytosis mechanisms outlined in Figure 2.

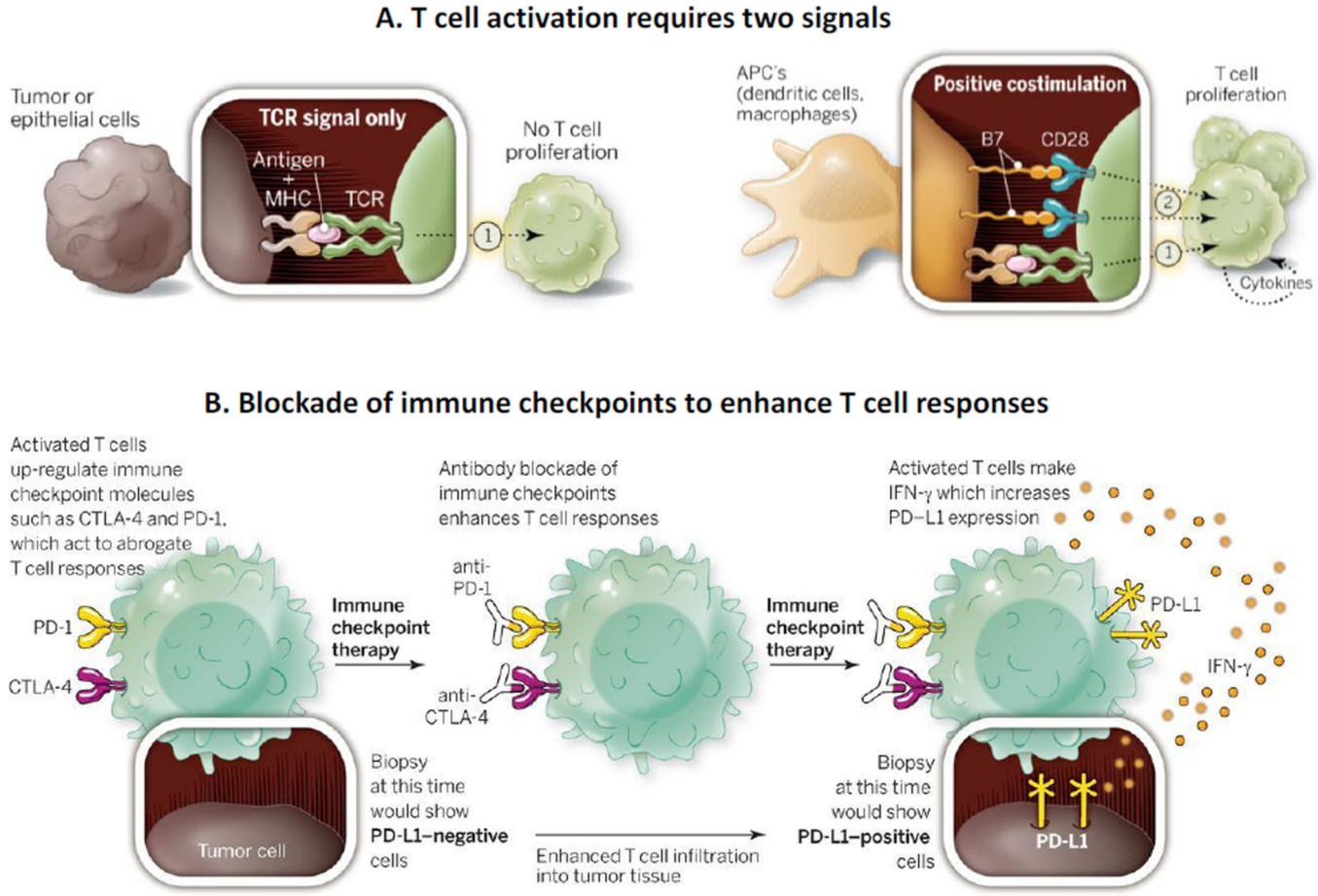

Figure 4. Immune checkpoint therapy: Pharmacological basis

A. T cell activation requires two signals. T cells recognize tumor antigens presented by the major histocompatibility complex (MHC) on the surface of cells through their T-cell receptor (TCR). This first signal (1) is insufficient to turn on a T-cell response, and a second signal (2) delivered by the B7 costimulatory molecules on antigen presenting cells (APC) is required for activation. **B. Blockade of immune checkpoints to enhance T cell responses**. After activation, T cells express immune checkpoints such as CTLA-4 and PD-1. They further secrete IFN-γ, which leads to expression of PD-L1 on tumor cells and inflammatory cells and causes inhibition of T cells upon interaction with PD-1. Blocking of immune checkpoints with antibodies prevents T cell inactivation and enhances T cell responses. The expression of PD-L1 on tumor cells may be absent in early biopsies obtained prior to immune checkpoint therapy but would be detectable after the therapy. Figure and legend are reprinted with permission from [221]. The legend was adjusted for the current discussion.

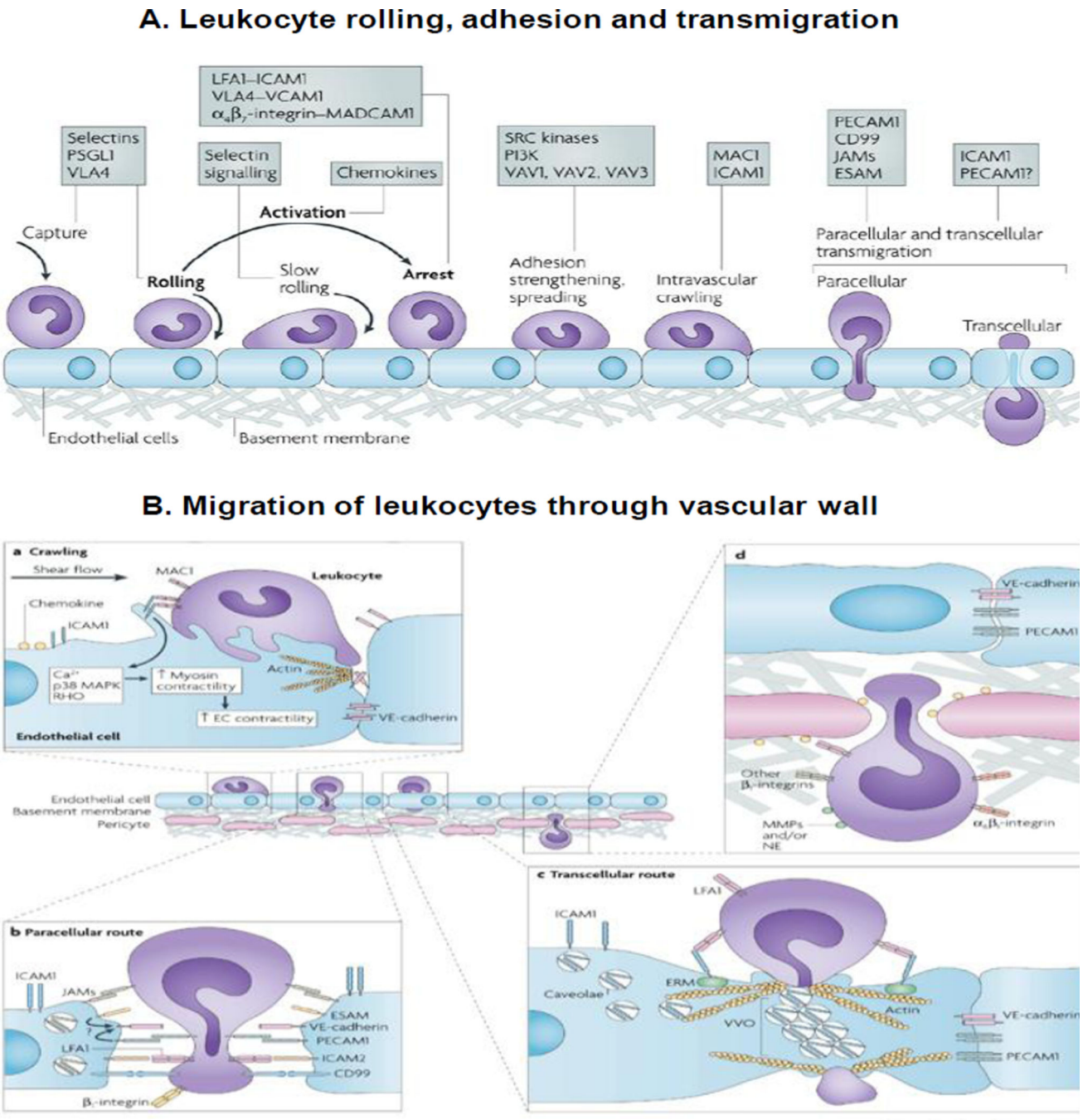

Figure 5. Trafficking of leukocytes to interstitial space

A. Leukocyte rolling, adhesion and transmigration. The original three steps are shown in bold: rolling, which is mediated by selectins, activation, which is mediated by chemokines, and arrest, which is mediated by integrins. Progress has been made in defining additional steps: capture (or tethering), slow rolling, adhesion strengthening and spreading, intravascular crawling, and paracellular and transcellular transmigration. Key molecules involved in each step are indicated in boxes. ESAM, endothelial cell-selective adhesion molecule; ICAM1, intercellular adhesion molecule 1; JAM, junctional adhesion molecule;

LFA1, lymphocyte function-associated antigen 1 (also known as $_{L2}$-integrin); MAC1, macrophage antigen 1; MADCAM1, mucosal vascular addressin cell-adhesion molecule 1; PSGL1, P-selectin glycoprotein ligand 1; PECAM1, platelet/endothelial-cell adhesion molecule 1; PI3K, phosphoinositide 3-kinase; VCAM1, vascular cell-adhesion molecule 1; VLA4, very late antigen 4 (also known as $_{41}$-integrin). **B. Migration of leukocytes through vascular walls.** This process involves penetrating the endothelial-cell barrier and its associated basement membrane and the pericyte sheath. (a) Extension of leukocyte membrane protrusions into the endothelial-cell body and endothelial-cell junctions is triggered by ligation of intercellular adhesion molecule 1 (ICAM1) by MAC1 (macrophage antigen 1). Ligation of ICAM1 is associated with increased intracellular Ca^{2+} and activation of p38 mitogen-activated protein kinase (MAPK) and RAS homologue (RHO) GTPase, which may collectively activate myosin light-chain kinase leading to enhanced endothelial-cell contraction and hence opening of inter-endothelial contacts. These events may promote leukocyte migration through endothelial junctions (paracellular route), although leukocyte migration can also occur through the body of the endothelium (transcellular route). Transmigration through the endothelium can also induce cell-surface expression of members of the $_{1}$-integrin family and proteases on neutrophils and other leukocytes that may facilitate the onwards movement of the leukocyte through the vessel wall. (b) Paracellular migration involves the release of endothelial-expressed vascular endothelial cadherin (VE-cadherin) and is facilitated by intracellular membrane compartments containing a pool of platelet/endothelial-cell adhesion molecule 1 (PECAM1) and possibly other endothelial-cell junctional molecules, such as junctional adhesion molecule A (JAM-A). Other molecules involved in paracellular transmigration are endothelial cell-selective adhesion molecule (ESAM), ICAM2 and CD99. (c) Transcellular migration occurs in 'thin' parts of the endothelium, and therefore there is less distance for a leukocyte to migrate. ICAM1 ligation leads to translocation of ICAM1 to actin- and caveolae-rich regions. ICAM1-containing caveolae link together forming vesiculo-vacuolar organelles (VVOs) that form an intracellular channel through which a leukocyte can migrate. Ezrin, radixin and moesin (ERM) proteins could act as linkers between ICAM1 and cytoskeletal proteins (such as actin and vimentin), causing their localization around the channel, thereby providing structural support for the cell under these conditions. (d) Migration through the endothelial basement membrane and pericyte sheath can occur through gaps between adjacent pericytes and regions of low protein deposition within the extracellular matrix. This response can be facilitated by $_{61}$-integrin and possibly proteases, such as matrix metalloproteinases (MMPs) and neutrophil elastase (NE). Figure and legend are reprinted with permission from [217].

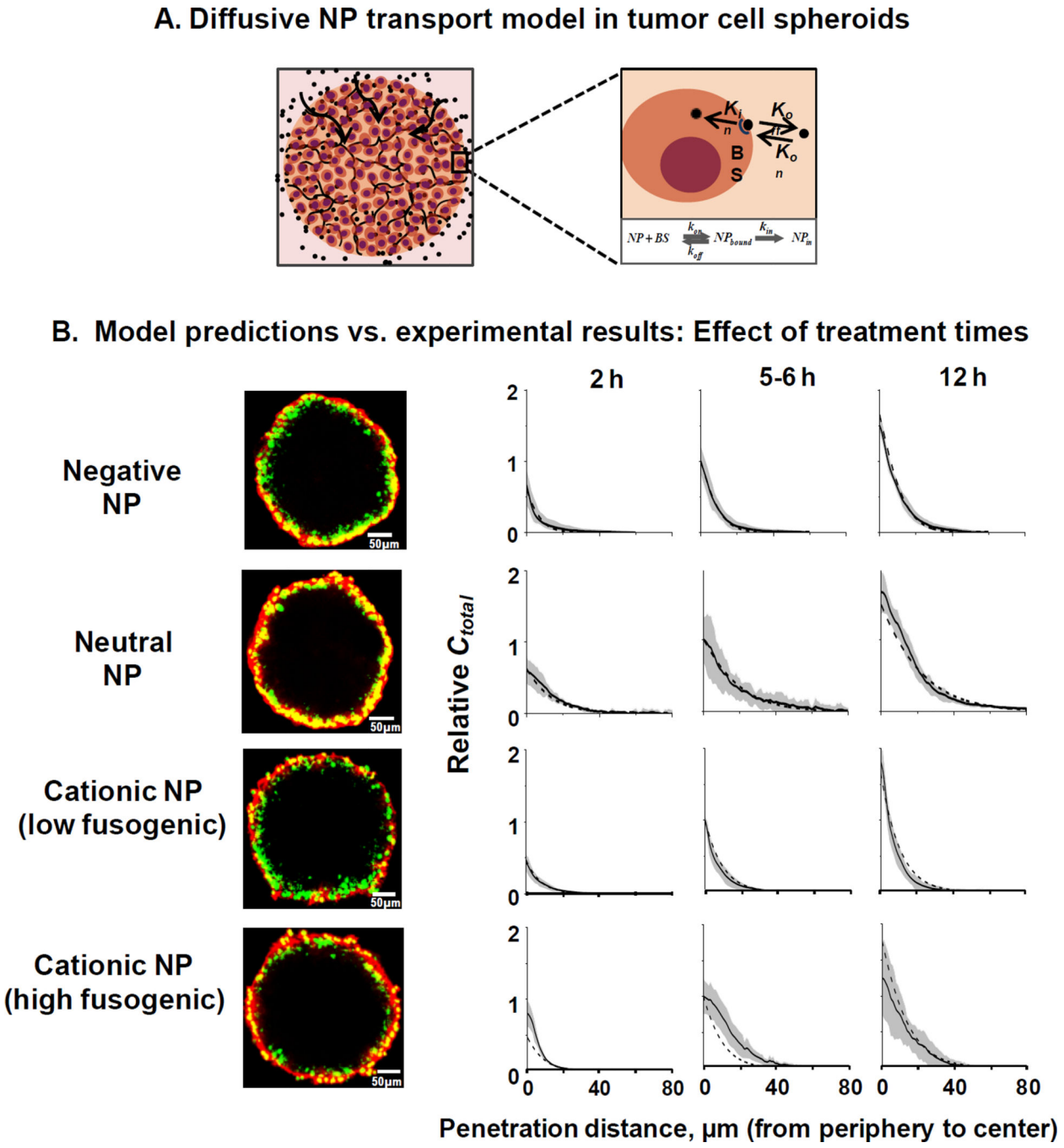

Figure 6. Predicting diffusive nanoparticle transport in 3-dimensional tumor cell spheroids

(A) Models of NP diffusion into spheroids. BS binding sites. **(B) Evaluation of model performance: Comparison of experimental results with model predictions.** Left: Confocal microscopic images of spheroids treated with negatively charged NP (polystyrene beads, 20 nm, −49.1 mV), near neutral NP (liposomes, 110 nm, −9.7 mV), positive liposome NP with low fusogenic content (135 nm, +36 mV, 1 mol% fusogenic lipid), and positive liposome NP with high fusogenic content (130 nm, +37.7 mV, 20 mol% fusogenic lipid). ×20 magnification. Red: NP. Green: nuclei. Yellow: overlapping nuclei and liposomes. The

results for predicting the effect of treatment times are shown. Similar model performance was found for predicting the effect of NP concentrations (not shown, available in cited reference). Spheroids were treated with a fixed initial NP concentration (18.8 nM for negative NP, 1.13 nM for near neutral liposomes, and 0.55 nM for both of the positively charged liposomes). 0.55 nM for C20-5 liposomes). Solid lines and shaded areas: experimentally observed profiles plus 95% confidence intervals. Dashed lines: model-simulated profiles. Relative total NP concentrations, C_{total} (sum of interstitial, cell-bound and internalized drug concentrations), are normalized to the levels of reference treatment groups (18.8 nM and 5 h for negative NP, 1.13 nM and 6 h for near neutral liposomes, and 0.55 nM and 6 h for positive liposomes). Bar, 50 μm. Figures and legends are adapted from [257, 258] and reprinted with permission.

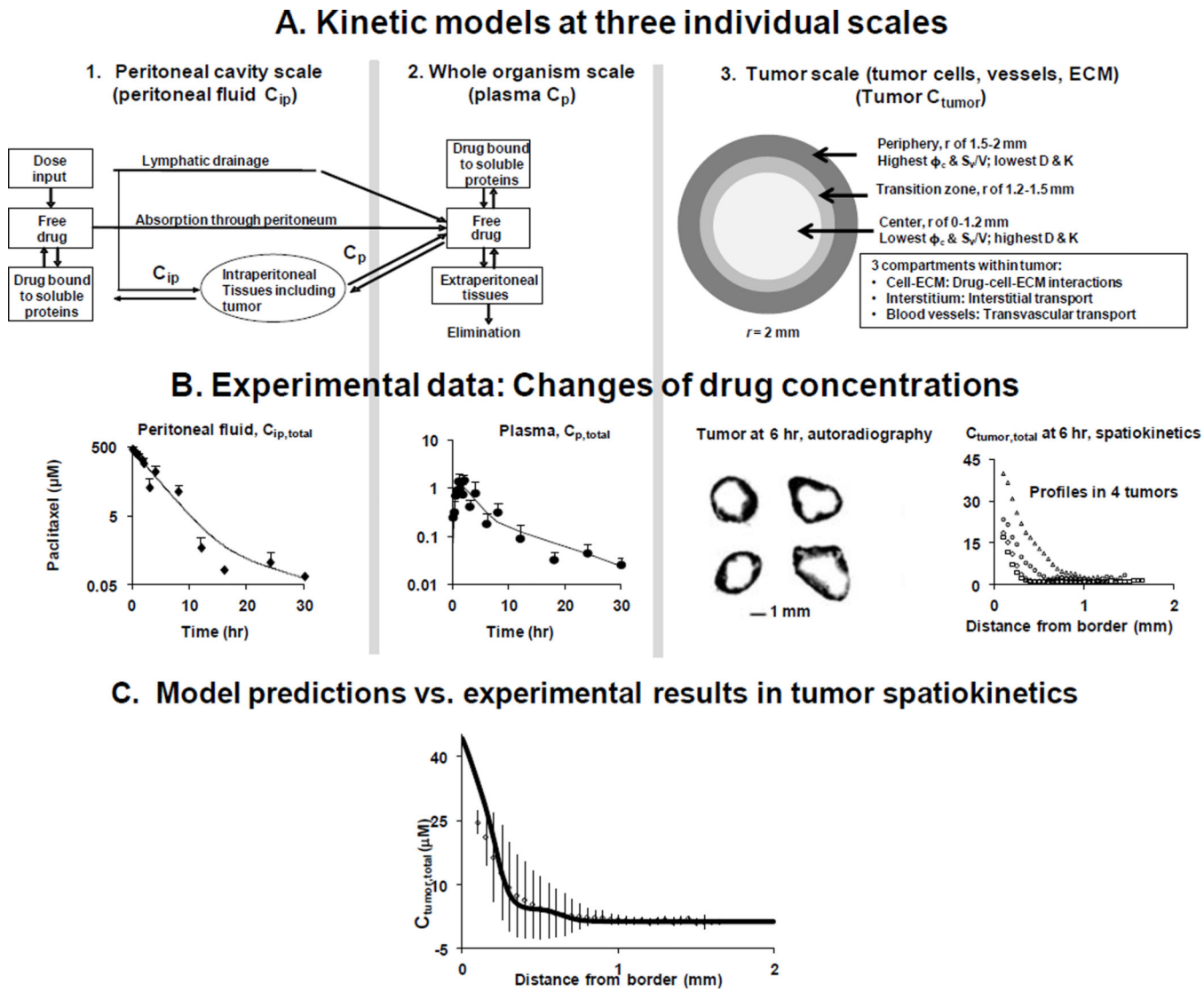

Figure 7. Multiscale models for intraperitoneal therapy

After an intraperitoneal injection, drug disposition in peritoneal tumors is determined by kinetic processes occurring on three scales. **A. Kinetic models at individual scales.** The models for the peritoneal cavity scale (left panel) and the whole organism scale (middle panel) describe the drug drainage by lymphatic system, drug absorption into blood circulation through peritoneal tissues, drug clearance from the body, drug redistribution to peripheral tissues including intraperitoneal and extraperitoneal tissues, drug binding to extracellular proteins and cells, and tissue-blood drug exchange. The model for the tumor scale (right panel) describes the transvascular and interstitial drug transport (by diffusion and convection, measured as diffusivity D and hydraulic conductivity K) and the intratumoral heterogeneities (in tumor cell density, vessel density and surface area, interstitial void volume; represented by terms such as φ_c, S_v/V). We assumed the geometry of a spherical tumor (4 mm in diameter) comprising three layers: necrotic center of 1.2-mm radius (white area), tumor periphery of 500-μm thickness (dark gray area), and the transition zone (light gray area). The three scales are connected per the transfer processes outlined in Figure 1 and

the tumor scale model used the drug concentration-time profiles in peritoneal fluid and systemic blood as the boundary conditions. **B. Experimental data of the time- or spatial-dependent changes in paclitaxel concentrations.** Mice were given an intraperitoneal injection of radiolabeled paclitaxel (10 mg/kg dissolved in 0.7 mL of 1:1 Cremophor/ethanol). Symbols are experimental data and lines are the best-fit lines to the kinetic models for peritoneal fluid (left panel) and for plasma (middle panel); note the different concentration scales. Solitary tumors were removed from four individual mice at 6 h and processed for autoradiograph. The tumor spatiokinetics, or changes in drug concentrations with the spatial positions, are shown (right panel). **C. Comparison of experimentally-observed and model-simulated spatiokinetics in tumors.** Symbols and bars: Average concentrations in four individual tumors plus one standard deviation at 6 h. Solid line: model-predicted tumor spatiokinetics profile. Figures and legends are adapted from Figures 1 and 5 in [259] and reprinted with permission.